J. Fluid Mech. (1983), *vol.* 131, *pp.* 427–454
Printed in Great Britain

The propagation of a voidage disturbance in a uniformly fluidized bed

By D. J. NEEDHAM AND J. H. MERKIN
Department of Applied Mathematical Studies, University of Leeds, Leeds LS2 9JT, England

(Received 8 November 1982)

By considering the evolution of a localized voidage disturbance imposed on an otherwise uniformly fluidized bed we are able to determine the dominant effects of the many terms in the continuum equations of motion governing a fluidized bed. For small perturbations a linearized theory is developed, showing that the stability of the uniform state is critically dependent upon the particle-phase collisional pressure and the flow rate of the uniform state, while the effect of particle phase viscosity is shown to be purely dispersive. When the uniform state is stable, the disturbance is shown to develop into a decaying pulse followed by a decaying wavetrain.

For finite-amplitude disturbance, nonlinear effects are considered. These are shown to give rise to the propagation of high voidage gradients through the bed. Having established that such voidage fronts will develop, a detailed study of their structure is made. This gives strong indications that, for flow rates at which the uniform state is unstable, the bed will restabilize into a quasisteady periodic state.

1. Introduction

Fluidization is a process in which a bed of solid particles, whose diameters range typically from 1 mm down to 10^{-2} mm, is subject to a vertical, upward flow of fluid. On increasing the fluid flow speed, a point is reached where the upward drag exerted by the fluid balances the downward gravitational force on the particles, which then become buoyant. At this point the bed is fluidized at minimum fluidizing velocity, exhibiting large-scale phenomena, such as buoyancy and surface waves, similar to those of a liquid. Because of the large surface area of contact between the two phases, the fluidized bed has found many industrial applications, for example in catalytic reactions, mixing and coating processes and the combustion of low-grade coals. In the majority of applications, fluidized beds are efficient only when the fluidization is homogeneous, i.e. when the voidage (the volume of fluid per unit volume of the two-phase medium) is uniform; however, it has been found that this situation is not always attainable, especially with gas-fluidized beds. Experimental work with gas-fluidized beds has shown that on increasing the flow rate above that of minimum fluidization the bed will expand uniformly, the voidage increasing uniformly, until a further critical flow rate is reached, after which the bed no longer expands uniformly, but develops voidage non-uniformities known as 'bubbles' or 'slugs'. Bubbling occurs in beds whose diameters are large compared with their height and is characterized by approximately spherical high-voidage regions propagating upwards through the bed, while slugging is found in narrow-diameter beds and is characterized by horizontal bands of high voidage propagating upwards through the bed by rapid particle raining from the sharp voidage fronts. Further details of the

behaviour of fluidized beds with increasing flow rates are given by Zenz (1971) and Richardson (1971).

Since bubbling and slugging are often undesirable for efficient operation, many theoretical studies have been aimed at describing and understanding the mechanisms involved in the development of such phenomena. The fundamental equations of motion governing a fluidized bed have been derived by considering the fluid and particle phases as interpenetrating continua; with detailed derivations being given by Anderson & Jackson (1967), Murray (1965), Garg & Pritchett (1975), and Homsy, El-Kaissey & Didwania (1980). The continuum equations of motion have been used by the above authors to study the linearized hydrodynamic stability of the uniformly fluidized state. These studies have been able to show primarily that gas-fluidized beds are in general more unstable than liquid-fluidized beds, but owing to the complexity of the resulting dispersion relation the mechanism of instability and the relative importance of the many terms in the equations of motion have not been revealed. A more recent study of the nonlinear effects has been given by Fanucci, Ness & Yen (1979), who, on neglecting particle-phase viscosity, reduced the equations of motion to a hyperbolic system which was then integrated numerically. Although their work did show the possibility of voidage discontinuities arising from continuous initial disturbances, it was limited to a sinusoidal initial disturbance and was unable to elucidate the fundamental mechanisms involved in the formation of such fronts. In fact, Murray (1965) neglected particle collisional pressure as being unimportant and predicted all gas-fluidized beds to be unstable at all flow rates, which would contradict experimental observation; while in this paper we demonstrate that particle collisional pressure has a strong stabilizing influence on the uniformly fluidized state. This has also been reported in the numerical study by Garg & Pritchett. Even when the particle collisional pressure is not sufficiently strong to stabilize the uniform state completely, it must still be included in a discussion of fluidization to give the flow the possibility of reaching a new, quasisteady equilibrium state, as it is one of the main dissipative mechanisms in the system curbing the unbounded growth of voidage perturbations.

In this paper we consider a simple initial-value problem in detail. This enables us to identify the mechanisms of fundamental importance in a fluidized bed in a rational manner. To simplify, attention is restricted to gas-fluidized beds in which $\rho_f/\rho_s \ll 1$ (where ρ_f is the fluid density and ρ_s is the solid density) and we consider only one-dimensional vertical flow; physically this corresponds to flow in a narrow-diameter fluidized bed. The evolution of a localized voidage disturbance in an otherwise uniformly fluidized bed is examined. For small perturbations a linear theory is developed which highlights the stabilizing effect of particle collisional pressure upon the uniform state. The resulting stability criterion is dependent both upon the effect of particle collisional pressure and the flow rate of the uniform state, and gives encouraging qualitative agreement with experimental observations reported by Zenz & Othmer (1960) on the behaviour of narrow-diameter gas-fluidized beds with increasing flow rates. For finite-amplitude disturbances, nonlinear effects are important. These give rise to the formation and propagation of high voidage gradients, and the growth of the instabilities of the linearized theory are shown to be curbed by the changing sign of a nonlinear diffusion coefficient. Since the propagation of high voidage gradients is recognized as playing an important role in the phenomena of slugging and bubbling, and, having determined that such fronts can develop, in the final part of the paper we isolate such fronts and examine their structure in some detail. This gives an indication that the bed may restabilize into a quasisteady

periodic state at flow rates for which the uniform state is unstable to small-amplitude disturbances.

2. Equations of motion

We are concerned with the one-dimensional (vertical) flow in fluidized beds in which $\rho_f \ll \rho_s$, where ρ_f is the fluid density and ρ_s is the solid density. When terms of order ρ_f/ρ_s are neglected, the equations of motion governing a fluidized bed are

$$\frac{\partial E}{\partial t}+\frac{\partial}{\partial x}(EU) = 0, \tag{1}$$

$$-\frac{\partial E}{\partial t}+\frac{\partial}{\partial x}[(1-E)\,V] = 0, \tag{2}$$

$$\rho_s(1-E)\left[\frac{\partial V}{\partial t}+V\frac{\partial V}{\partial x}\right] = B(E)\,(U-V)-(1-E)\rho_s g-\frac{\partial P_s}{\partial x}+\bar{\mu}_s\frac{\partial^2 V}{\partial x^2}, \tag{3}$$

$$\frac{\partial P}{\partial x} = -B(E)\,(U-V). \tag{4}$$

Here x is the coordinate measuring distance vertically upwards, t is time, U is fluid velocity, V is particle velocity, E is voidage (volume of fluid per unit volume of the two-phase system), P is fluid-phase pressure, $P_s(E)$ is particle-phase pressure, $B(E)$ is the drag coefficient per unit bed volume and $\bar{\mu}_s$ is the viscosity of the particle phase. Equations (1) and (2) are continuity equations for the fluid and particle phases respectively. Equation (3) comes from a momentum balance in the particle phase. The first term on the right-hand side represents the drag on the particles exerted by the fluid; the second term is the gravitational force on the particles, the third term represents interparticle pressure (generated by collisions in the particle phase); the final term represents viscosity effects in the particle phase. Equation (4) comes from a momentum balance in the fluid phase (fluid inertia and viscosity being neglected since we are considering gas-fluidized beds, for which $\rho_f/\rho_s \ll 1$). This last equation serves only to determine P (E, V and U being first determined by solution of (1)–(3)), and can henceforth be removed from the discussion.

To close the set of equations (1)–(3) it remains to relate the drag coefficient per unit volume $B(E)$ and the particle-phase pressure $P_s(E)$ to voidage. $B(E)$ may be written as $B(E) = (1-E)\,D(E)/V_p E$, where V_p is the volume of one particle and $D(E)$ is now the drag coefficient for one particle, and, following Murray (1965), is a decreasing function of voidage E, with functional form

$$D(E) = D_0 E^{-(n-1)}. \tag{5}$$

D_0 is the Stokes drag on a single particle and $n > 1$ (n is not necessarily an integer). This form is chosen to satisfy the condition $D(E)\to D_0$ as $E\to 1$, and is suggested by the uniform-bed expansion correlation given by Richardson (1971), which for gas-fluidized beds suggests a value of $n \approx 3$. All the work available at present (e.g. Saffman 1973) on the calculation of $D(E)$ is confined to the case of very high voidage, which limit is not really applicable to the study of fluidized beds. Consequently, to fix the functional form of $D(E)$ over a wide range of values of E, reliance has to be placed on correlations of experimentally determined results.

Drew & Segal (1971) suggest that the collisional pressure in the particle phase P_s is a decreasing function of voidage. In view of the little experimental evidence

available relating interparticle pressure to voidage, we take, as a first approximation, the simple linear form which reduces to zero as $E \to 1$, namely

$$P_s(E) = P_0(1-E), \tag{6}$$

where P_0 is a constant, having dimensions of pressure, and is of the order of 10 dyn/cm^2 to be consistent with values used by Anderson & Jackson (1968).

A state of fluidization is essentially a balance between the upward drag on the particle phase, induced by the vertical flow of fluid through the bed, and the downward gravitational force acting on the particle phase. The drag, and hence the drag coefficient, is therefore expected to play an important role in determining the behaviour within a fluidized bed. The effect of collisional pressure in the particle phase is also shown in this paper to play a vital role in stabilizing a fluidized bed. Although, to close the equations of motion, functional forms for the dependence of the drag coefficient and collisional pressure are needed, and specific forms have been proposed in (5) and (6), it is expected that the behaviour will not be affected, qualitatively at least, for alternative functional forms, provided the overall trend of monotonic decrease with increasing voidage and the appropriate limits as $E \to 1$ are satisfied.

A further simplification can be made by adding (1) and (2) and integrating with respect to x. This yields the equation

$$EU + (1-E)\,V = M(t). \tag{7}$$

$M(t)$ is a function only of time. Equation (7) then is used to replace (1). It should be noted that the left hand side of (7) is the total volumetric flow per unit cross-sectional area, and, in accordance with the incompressibility of the whole system, (7) shows that the volume flow is independent of x.

The simplest solution to (7), (2) and (3) is one that represents a state of uniform fluidization (or homogeneous fluidization), in which the particle phase velocity is everywhere zero, the fluid-phase velocity is a constant U_0 and the voidage is a constant ϵ_0. Substitution into (2), (3) and (7) yields the compatibility relations

$$\epsilon_0 U_0 = M_0, \tag{8}$$

$$B(\epsilon_0)\,U_0 = (1-\epsilon_0)\,\rho_s g. \tag{9}$$

For a given volume flow M_0, (8) and (9) determine U_0 and ϵ_0. Using (5), (9) can be written in the explicit form

$$U_0 = U_t \epsilon_0^n, \tag{10}$$

where U_t is, under the assumption $\rho_f/\rho_s \ll 1$, the terminal free-fall velocity of a single particle in the stationary fluid. Equation (10) is Richardson's correlation for the expansion of uniformly fluidized beds.

In this paper we discuss the evolution of a localized voidage disturbance imposed on the uniform state at $t = 0$. A typical velocity scale is U_0 and lengthscale h, the spread of the initial disturbance. Using U_0 and h, non-dimensional quantities are introduced as follows:

$$U = U_0 \bar{U}, \quad V = U_0 \bar{V}, \quad x = h\bar{x}, \quad t = \frac{h}{U_0}\bar{t}, \quad P_s = \rho_s U_0^2 \bar{P}_s,$$

$$B(E) = \frac{\rho_s U_0}{h}\bar{B}(E), \quad M = \bar{M} U_0.$$

Substituting into (2), (3) and (7), and dropping bars for convenience, the equations in dimensionless form become

$$EU + (1-E)\,V = M, \tag{11}$$

$$-\frac{\partial E}{\partial t}+\frac{\partial}{\partial x}[(1-E)\,V]=0, \tag{12}$$

$$(1-E)\left[\frac{\partial V}{\partial t}+V\frac{\partial V}{\partial x}\right]=\bar{B}(E)\,(U-V)-\frac{1-E}{F}-\frac{\partial \bar{P}_s}{\partial E}\frac{\partial E}{\partial x}+\frac{1}{R}\frac{\partial^2 V}{\partial x^2}. \tag{13}$$

Here $F=U_0^2/gh$ is the Froude number and $R=\rho_s U_0 h/\bar{\mu}_s$ is the particle-phase Reynolds number. Using (5) and (6) we have $\bar{B}(E)=[(1-E)/F](\epsilon_0/E)^n$ and $\bar{P}_s(E)=\bar{P}_0(1-E)$, where $\bar{P}_0=(P_0/\rho_s U_0^2)$.

We consider the one-dimensional motion in an infinite fluidized region, which for $t<0$ is assumed uniformly fluidized (i.e. $U=1, V=0, E=\epsilon_0$). At $t=0$ a localized voidage disturbance is made upon the uniform state, with amplitude α. The initial conditions are

$$E(x,0)=\epsilon_0+\alpha g(x), \tag{14}$$

$$V(x,0)=0, \tag{15}$$

together with the conditions $U\to 1, V\to 0, E\to\epsilon_0$ far away from the disturbance, which determine M as a constant, M_0, where $M_0=\epsilon_0$. For a typical gas-fluidized bed, experimental results given by Richardson (1971) show that certainly for particles with diameters of the order of 10^{-2} mm $U_0^2\ll gh$ for all lengthscales h covered by the continuum theory. However, for mineral particles with diameters in the upper range, of the order of 1 mm, the fluidizing velocity can be of the order of 20 cm/s. The value of h for which the assumption $U_0^2\ll gh$ is justified is then somewhat larger, the theory then approaching a long-wave theory. Throughout the rest of the paper we therefore assume $F\ll 1$, while the particle-phase Reynolds number R is typically $O(1)$. We consider first the linearized problem when $|\alpha|\ll 1$.

3. The linearized problem $|\alpha|\ll 1$

When $|\alpha|\ll 1$, we look for a solution of (11)–(13) in the form

$$\left.\begin{aligned} E(x,t)&=\epsilon_0+\alpha\bar{E}(x,t),\\ V(x,t)&=\alpha\bar{V}(x,t),\\ U(x,t)&=1+\alpha\bar{U}(x,t). \end{aligned}\right\} \tag{16}$$

When (16) is substituted into (11)–(13), and terms of $O(\alpha^2)$ are neglected, we obtain a set of linear partial differential equations for the perturbed quantities $\bar{E}$, $\bar{V}$ and $\bar{U}$; namely

$$\epsilon_0\bar{U}+\bar{E}+(1-\epsilon_0)\,\bar{V}=0, \tag{17}$$

$$\frac{\partial\bar{E}}{\partial t}=(1-\epsilon_0)\frac{\partial\bar{V}}{\partial x}, \tag{18}$$

$$(1-\epsilon_0)\frac{\partial\bar{V}}{\partial t}=\left(\frac{1}{F}+\bar{B}_0'\right)\bar{E}+\bar{B}_0(\bar{U}-\bar{V})-\bar{P}_s'|_{\epsilon_0}\frac{\partial\bar{E}}{\partial x}+\frac{1}{R}\frac{\partial^2\bar{V}}{\partial x^2},$$

where the constants are

$$\left.\begin{aligned} \bar{B}_0&\equiv\bar{B}(\epsilon_0)=\frac{1-\epsilon_0}{F},\\ B_0'&\equiv\left.\frac{\mathrm{d}\bar{B}}{\mathrm{d}E}\right|_{\epsilon_0}=-\frac{n-(n-1)\epsilon_0}{F\epsilon_0}, \quad \bar{P}_s'|_{\epsilon_0}=\left.\frac{\mathrm{d}\bar{P}_s}{\mathrm{d}E}\right|_{\epsilon_0}=-\bar{P}_0. \end{aligned}\right\} \tag{19}$$

The initial and boundary conditions become

$$\bar{E}(x,0)=g(x), \quad \bar{V}(x,0)=0, \quad \bar{E},\bar{V},\bar{U}\to 0 \quad \text{far away from the disturbance.} \tag{20}$$

To obtain a single equation for the voidage perturbation $\bar{E}$, (17) is first used to eliminate $\bar{U}$ from (19). The resulting equation is then differentiated with respect to x, and on using (18) to eliminate $\bar{V}$, the equation becomes

$$F\frac{\partial^2\bar{E}}{\partial t^2} = -A\frac{\partial\bar{E}}{\partial x} - B\frac{\partial\bar{E}}{\partial t} + F\bar{P}_0\frac{\partial^2\bar{E}}{\partial x^2} + FC\frac{\partial^3\bar{E}}{\partial x^2\,\partial t}, \tag{21}$$

where A, B and C are positive constants given by

$$A = \frac{(n+1)(1-\epsilon_0)}{\epsilon_0}, \quad B = \frac{1}{\epsilon_0}, \quad C = \frac{1}{R(1-\epsilon_0)}.$$

To solve (21), we require a further condition on $\bar{E}$ at $t = 0$. This is provided by (18) as

$$\left.\frac{\partial\bar{E}}{\partial t}\right|_{t=0} = 0. \tag{22}$$

Since $F \ll 1$ it is natural to look for a solution of (21) by expanding $\bar{E}(x,t)$ in powers of F:

$$\bar{E}(x,t) = \bar{E}_0(x,t) + \bar{E}_1(x,t)\,F + \bar{E}_2(x,t)\,F^2 + O(F^3). \tag{23}$$

A problem arises immediately. The equation for $\bar{E}_0$ is

$$\frac{\partial\bar{E}_0}{\partial t} + \frac{A}{B}\frac{\partial\bar{E}_0}{\partial x} = 0. \tag{24}$$

Clearly the solution of (24) can be made to satisfy only one of the two initial conditions. This difficulty arises because of the neglect of the term $F\partial^2\bar{E}/\partial t^2$. To overcome this difficulty we solve in two regions: an outer region, where $t = O(1)$, and an inner region where $t = O(F)$ and the second-order time derivative is retained at leading order. Defining inner variables

$$\hat{t} = tF^{-1}, \quad \bar{E} \equiv \bar{E}_{\mathrm{I}}(x,\hat{t}), \tag{25}$$

and substituting into (21), leads to the inner equation

$$\frac{\partial^2\bar{E}_{\mathrm{I}}}{\partial\hat{t}^2} = -AF\frac{\partial\bar{E}_{\mathrm{I}}}{\partial x} - B\frac{\partial\bar{E}_{\mathrm{I}}}{\partial\hat{t}} + F^2\bar{P}_0\frac{\partial^2\bar{E}_{\mathrm{I}}}{\partial x^2} + FC\frac{\partial^3\bar{E}_{\mathrm{I}}}{\partial x^2\,\partial\hat{t}}, \tag{26}$$

and now it is possible to impose both initial conditions $\bar{E}_{\mathrm{I}}(x,0) = g(x)$ and $\partial\bar{E}_{\mathrm{I}}/\partial\hat{t}|_{\hat{t}=0} = 0$. A solution of (26) is sought in the form

$$\bar{E}_{\mathrm{I}}(x,\hat{t}) = \bar{e}_0(x,\hat{t}) + \bar{e}_1(x,\hat{t})\,F + \bar{e}_2(x,\hat{t})\,F^2 + O(F^3). \tag{27}$$

Substitution of (27) into (26) leads to a hierarchy of equations, which can be solved in turn. This yields the inner solution as

$$\bar{E}_{\mathrm{I}}(x,\hat{t}) = g(x) + \left[\frac{Ag'(x)}{B^2}(1-\mathrm{e}^{-B\hat{t}}) - \frac{A}{B}g'(x)\,\hat{t}\right]F + O(F^2), \tag{28}$$

where primes denote differentiation with respect to x. Using the inner solution (28) and applying the matching principle, we find that the first two terms of the outer expansion, (23), must satisfy

$$\bar{E}_0(x,0) = g(x), \quad \bar{E}_1(x,0) = \frac{A}{B^2}g'(x). \tag{29}$$

Also we notice that since (24) has the general solution $\bar{E}_0(x-(A/B)\,t)$ it is convenient

to introduce a new variable $z = x-(A/B)t$. In terms of z and t, (21) becomes

$$B\frac{\partial \bar{E}}{\partial t} = F\left[\left(\bar{P}_0-\frac{A^2}{B^2}\right)\frac{\partial^2 \bar{E}}{\partial z^2}-\frac{AC}{B}\frac{\partial^3 \bar{E}}{\partial z^3}+C\frac{\partial^3 \bar{E}}{\partial z^2\,\partial t}+\frac{2A}{B}\frac{\partial^2 \bar{E}}{\partial z\,\partial t}-\frac{\partial^2 \bar{E}}{\partial t^2}\right]. \tag{30}$$

A solution of (30) is sought in the form

$$\bar{E}(z,t) = \bar{E}_0(z,t)+\bar{E}_1(z,t)\,F+\bar{E}_2(z,t)\,F^2+O(F^3). \tag{31}$$

Substitution of (31) into (30) leads to a hierarchy of equations for $\bar{E}_0, \bar{E}_1, \ldots$ to be solved, subject to the conditions (29). We find that

$$\bar{E}(z,t) = g(z)+\left[\frac{1}{B}\left\{\left(\bar{P}_0-\frac{A^2}{B^2}\right)g''(z)-\frac{AC}{B}g'''(z)\right\}t+\frac{A}{B^2}g'(z)\right]F+O(F^2). \tag{32}$$

An examination of (32) shows that the expansion is not uniformly valid as $t\to\infty$, because of the appearance of secular terms in the expansion. These will no longer be small corrections to the leading-order term when $t = O(F^{-1})$. To remove this non-uniformity and examine the behaviour when $t = O(F^{-1})$, we introduce a new 'independent', slow time variable $\tau = Ft$, and assume $\bar{E} = \bar{E}(z,t,\tau)$. The method of multiple scales is now used (Nayfeh 1973). Introducing the slow time variable into (30) leads to

$$\begin{aligned}B\left(\frac{\partial \bar{E}}{\partial t}+F\frac{\partial \bar{E}}{\partial \tau}\right) = F\Bigg[&\left(\bar{P}_0-\frac{A^2}{B^2}\right)\frac{\partial^2 \bar{E}}{\partial z^2}-\frac{AC}{B}\frac{\partial^3 \bar{E}}{\partial z^3}+C\frac{\partial^3 \bar{E}}{\partial z^2\,\partial t}+FC\frac{\partial^3 \bar{E}}{\partial z^2\,\partial \tau}\\&+\frac{2A}{B}\frac{\partial \bar{E}}{\partial z\,\partial t}+\frac{2AF}{B}\frac{\partial^2 \bar{E}}{\partial z\,\partial \tau}-\frac{\partial^2 \bar{E}}{\partial t^2}-F^2\frac{\partial^2 \bar{E}}{\partial \tau^2}-2F\frac{\partial^2 \bar{E}}{\partial t\,\partial \tau}\Bigg].\end{aligned} \tag{33}$$

A solution of (33) is again sought in the form of the expansion (31), except that now the $\bar{E}_i \equiv \bar{E}_i(z,t,\tau)$. Substituting into (33) and equating powers of F, we find that, to remove secular terms from the $O(F)$ correction, the leading-order term must satisfy

$$B\frac{\partial \bar{E}_0}{\partial \tau} = \left(\bar{P}_0-\frac{A^2}{B^2}\right)\frac{\partial^2 \bar{E}_0}{\partial z^2}-\frac{AC}{B}\frac{\partial^3 \bar{E}_0}{\partial z^3}, \tag{34}$$

together with the first of the initial conditions (29).

It is now clear from (34) that the source of possible instability comes from a 'concentrating' of voidage due to a negative diffusion coefficient. The coefficient of the diffusion term, $\bar{P}_0-A^2/B^2$, is dependent upon the particle collisional pressure, through $\bar{P}_0$, and the uniform voidage ϵ_0 (and hence the volume flow at uniform fluidization). The importance of the inclusion of particle-phase collisional pressure is now obvious. Neglect of this effect (i.e. putting $\bar{P}_0 \equiv 0$) will always lead to the prediction of unstable (to small-amplitude disturbances) uniform states at all flow rates (cf. e.g. Murray 1965). However, it is observed experimentally in the fluidization of small particles (of diameters less than about 0.1 mm), where the interparticle collisional pressure is relatively large, that there is a range of flow rates over which gas-fluidized beds behave uniformly, and can be expanded uniformly with increasing flow rate, as, for example, in results reported by Richardson (1971). Therefore (34) emphasizes that particle-phase collisional pressure is not a negligible effect, and must be included in any attempt to construct predictive models of a fluidized bed. We can also infer immediately from (34) that since the effect of particle-phase viscosity appears only in the final term it gives rise just to dispersive effects, and that dispersion and diffusion (positive or negative) take place over a timescale $O(1/F)$.

The dispersion relation for (34) is found by substituting $\bar{E}_0 = A(k)\,\mathrm{e}^{\mathrm{i}kx-\mathrm{i}\omega\tau}$, which gives

$$\omega(k) = -\mathrm{i}\left(\bar{P}_0 - \frac{A^2}{B^2}\right)k^2 - \frac{AC}{B^2}k^3. \tag{35}$$

Then by Fourier's theorem, and applying the condition (29), the uniformly valid outer solution, to leading order, is given by

$$\bar{E}_0(z,\tau) = \frac{1}{2\pi}\int_{-\infty}^{\infty}\left[\int_{-\infty}^{\infty} g(s)\,\mathrm{e}^{-\mathrm{i}ks}\,\mathrm{d}s\right]\exp\left[\mathrm{i}kz + \frac{AC}{B^2}\mathrm{i}k^3\tau - \frac{\bar{P}_0 - A^2/B^2}{B}k^2\tau\right]\mathrm{d}k. \tag{36}$$

Clearly the integral in (36) is unbounded in the unstable case $\bar{P}_0 < A^2/B^2$. In the stable case when $\bar{P}_0 \geqslant A^2/B^2$, it may be evaluated asymptotically as $\tau \to \infty$ using the method of steepest descents. Introducing new constants $a_1 = AC/B^2$ and $a_2 = (\bar{P}_0 - A^2/B^2)/B$ and putting $\tilde{z} = z + (a_2^2/3a_1)\tau$ we find that, as $\tau \to \infty$, with $\tilde{z}/\tau$ held constant, the asymptotic behaviour of (36) is given by

$$\left.\begin{aligned}
\bar{E}_0(\tilde{z},\tau) &\sim \frac{\bar{H}(U_0)\,(3a_1)^{\frac{1}{2}}}{(2\pi)^{\frac{1}{2}}\,|\tilde{z}|^{\frac{1}{4}}\,\tau^{\frac{1}{4}}}\exp\left(-\frac{a_2^3\tau}{27a_1^2}\right)\exp\left(-\frac{\tilde{z}}{3a_1}\left[\frac{2}{3}\left(\frac{\tilde{z}}{\tau}\right)^{\frac{1}{2}} - a_2\right]\right) \quad (\tilde{z} > 0), \\
\bar{E}_0(\tilde{z},\tau) &\sim \frac{2\bar{H}(U_1)\,(3a_1)^{\frac{1}{2}}}{(2\pi)^{\frac{1}{2}}\,|\tilde{z}|^{\frac{1}{4}}\,\tau^{\frac{1}{4}}}\exp\left(-\frac{a_2^3\tau}{27a_1^2}\right)\exp\left(\frac{a_2}{3a_1}\tilde{z}\right)\sin\left\{\frac{2}{3}\frac{\tilde{z}}{(3a_1)}\left(\frac{\tilde{z}}{\tau}\right)^{\frac{1}{2}}\right\} \quad (\tilde{z} < 0),
\end{aligned}\right\} \tag{37}$$

where $\bar{H}$ is the Fourier transform of $g(x)$, and $U_0 = \{(1/3a_1)\,(\tilde{z}/\tau + a_2^2/3a_1)\}^{\frac{1}{2}}$, $U_1 = \mathrm{i}\{(1/3a_1)\,|\tilde{z}/\tau + a_2^2/3a_1|\}^{\frac{1}{2}}$. The asymptotic behaviour (37) shows the initial disturbance develops into a decaying pulse, centred at $\tilde{z} \approx 0$, followed by a decaying wavetrain.

It is now straightforward to obtain the appropriate inner and outer expansions for the perturbed fluid and solid velocities $\bar{U}$ and $\bar{V}$ respectively, from (17) and (18). We find that the inner solutions are

$$\begin{aligned}
\bar{V}_1(x,\tilde{t}) &= -\frac{Ag(x)}{B(1-\epsilon_0)}(1-\mathrm{e}^{-B\tilde{t}}) + O(F), \\
\bar{U}_1(x,\tilde{t}) &= -\frac{g(x)}{\epsilon_0}\left(1 - \frac{A}{B}[1-\mathrm{e}^{-B\tilde{t}}]\right) + O(F).
\end{aligned} \tag{38}$$

These show that particle- and fluid-phase velocities adjust rapidly from their initial values on a timescale $O(F)$; (38) shows the rapid adjustment of the particle velocity from the initial value of zero, as the particles begin to fall through the higher-voidage region created at $t = 0$. This is the mechanism by which the higher-voidage region propagates through the bed. The outer solutions are

$$\bar{V}(z,\tau) = \frac{A}{2\pi B(1-\epsilon_0)}\int_{-\infty}^{\infty}\left[\int_{-\infty}^{\infty} g(s)\,\mathrm{e}^{-\mathrm{i}ks}\,\mathrm{d}s\right]\exp\left\{\mathrm{i}kz + \frac{AC\mathrm{i}k^3\tau}{B^2} - \frac{(\bar{P}_0 - A^2/B^2)\,k^2\tau}{B}\right\}\mathrm{d}k, \tag{39a}$$

$$\bar{U}(z,\tau) = \frac{-(1-A/B)}{2\pi\epsilon_0}\int_{-\infty}^{\infty}\left[\int_{-\infty}^{\infty} g(s)\,\mathrm{e}^{-\mathrm{i}ks}\,\mathrm{d}s\right] \times \exp\left\{\mathrm{i}kz + \frac{AC\mathrm{i}k^3\tau}{B^2} - \frac{(\bar{P}_0 - A^2/B^2)\,k^2\tau}{B}\right\}\mathrm{d}k + O(F), \tag{39b}$$

which, as with (36), can be evaluated asymptotically as $\tau \to \infty$ for the stable case $\bar{P}_0 \geqslant A^2/B^2$.

It is possible to derive (34) using a less formal technique than that outlined above.

Equation (21) gives to leading order the relationship

$$\frac{\partial}{\partial t} \approx \frac{-A}{B}\frac{\partial}{\partial x}. \tag{40}$$

Making this replacement for all time derivatives, except that of leading order, in (21), we obtain the following equation governing voidage variations:

$$\frac{\partial \bar{E}}{\partial t}+\frac{A}{B}\frac{\partial \bar{E}}{\partial x}=\frac{F}{B}\left\{\left(\bar{P}_0-\frac{A^2}{B^2}\right)\frac{\partial^2 \bar{E}}{\partial x^2}-\frac{AC}{B}\frac{\partial^3 \bar{E}}{\partial x^3}\right\},$$

which is exactly (34), when written in terms of z and τ. We illustrate this technique here, as a similar procedure will subsequently be used to derive the equation governing the nonlinear behaviour of voidage.

Finally, we show the stability condition derived for $F \ll 1$ (i.e. $U_0^2 \ll gh$) by the full solution of the initial-value problem is, in fact, valid for all values of F, not necessarily small. We look for exponential solutions of (21) in the form

$$\bar{E}_k(x,t) = \hat{E}(k)\,\mathrm{e}^{\mathrm{i}kx-qt}. \tag{41}$$

The substitution of (41) into (21) leads to the algebraic equation

$$q^2-\left\{B+\frac{Fk^2}{R}\right\}\frac{q}{F}+\frac{Aik}{F}+\bar{P}_0k^2=0. \tag{42}$$

Writing $q(k)=\xi(k)+\mathrm{i}\eta(k)$ and equating real and imaginary parts yields the two equations for ξ and η:

$$2\xi\eta+b\eta+C_\mathrm{i}=0, \tag{43a}$$

$$\xi^2+b\xi+C_\mathrm{r}-\eta^2=0, \tag{43b}$$

where $b=-(B+Fk^2/R)/F<0$; $C_\mathrm{r}=\bar{P}_0k^2\geqslant 0$; $C_\mathrm{i}=Ak/F$. Elimination between (43a) and (43b) leads to one fourth-order polynomial with real coefficients for $\xi(k)$, namely

$$Pn(\xi)\equiv(\xi^2+b\xi+C_\mathrm{r})\,(2\xi+b)^2-C_\mathrm{i}=0.$$

The uniform state will be stable provided that $\xi(k)>0$ for all k. Examination of the turning points of $Pn(\xi)$ shows them all to be at points ξ_i, where $\xi_i>0$. Now if ξ_1 is the smallest of these, then, since $\xi_1>0$ and $Pn(\xi)\to\infty$ as $\xi\to-\infty$, $Pn(\xi)$ is a monotonically decreasing function of ξ for $-\infty<\xi<\xi_1$, and hence for $-\infty<\xi\leqslant 0$. So a necessary and sufficient condition that all the real roots (there are two) of Pn are positive is $Pn(0)>0$. This yields the inequality $\bar{P}_0>A^2/(B+Fk^2/R)^2$, and, since this must hold for all k, we get the stability condition $\bar{P}_0>A^2/B^2$, previously derived.

We now examine the stability criterion in more detail. Using the expressions for A and B we have shown that the uniform state is stable provided that $\bar{P}_0>\{(n+1)\,(1-\epsilon_0)\}^2$. Now $\bar{P}_0=\bar{P}_0(\epsilon_0)=P_0/\rho_\mathrm{s}\epsilon_0^{2n}U_\mathrm{t}^2$, so, if we define $\tilde{P}_0$ by $\tilde{P}_0=\epsilon_0^{2n}\bar{P}_0=P_0/\rho_\mathrm{s}U_\mathrm{t}^2$, then $\tilde{P}_0$ is a function only of the material properties of the solid particles. In terms of $\tilde{P}_0$, the stability criterion becomes

$$\tilde{P}_0>\{(n+1)\,\epsilon_0^n(1-\epsilon_0)\}^2. \tag{44}$$

The right-hand side of (44) has just the two roots at $\epsilon_0=0$ and $\epsilon_0=1$, and for $0<\epsilon_0<1$, has just one turning point, namely a local maximum at $\epsilon_0=n(n+2)^{-1}$. If $\tilde{P}_0>\{(n+1)\,\epsilon_0^n(1-\epsilon_0)\}^2_{\max}$ then the uniform state is stable at all flow rates $M_0\,(=\epsilon_0)$, $0<M_0<1$. Very few gas-fluidized beds expand uniformly over the whole range of flow rates before transport, although it has been reported that this can happen when the particle phase has consisted of very fine powder. It is much more likely that

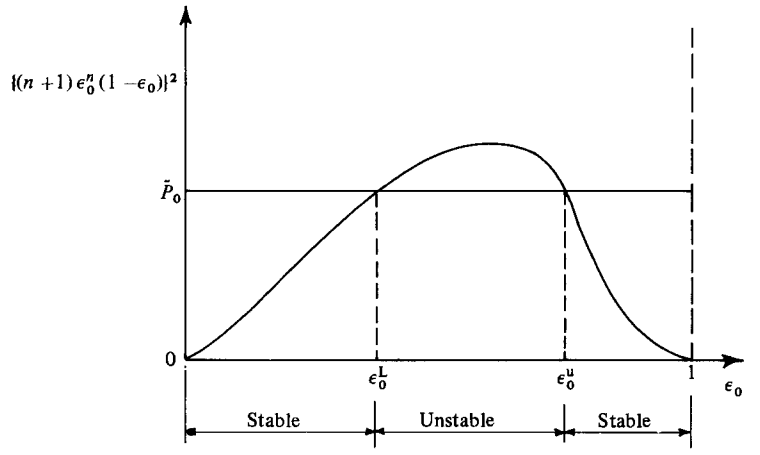

FIGURE 1. The stability condition for the uniform state with voidage ϵ_0.

$\tilde{P}_0 < \{(n+1)\epsilon_0^n(1-\epsilon_0)\}^2_{\max}$. In this case the equation $\tilde{P}_0 - \{(n+1)\epsilon_0^n(1-\epsilon_0)\}^2 = 0$ has two roots for $0 \leqslant \epsilon_0 \leqslant 1$, which we call ϵ_0^{u} and ϵ_0^{L}, where $\epsilon_0^{\mathrm{u}} > \epsilon_0^{\mathrm{L}}$. Thus, if the flow rate of the uniform state is such that $\epsilon_0 \leqslant \epsilon_0^{\mathrm{L}}$ or $\epsilon_0 \geqslant \epsilon_0^{\mathrm{u}}$, then it is stable to small-amplitude disturbances; otherwise it is unstable. For a given bed (i.e. $\tilde{P}_0$ and n fixed) a qualitative sketch of the stability condition (44) is illustrated in figure 1. The qualitative form compares well with experimental results for the behaviour of narrow-diameter gas-fluidized beds with increasing flow rates, reported by Zenz & Othmer (1960).

The propagation speed of the disturbance can now be determined. The 'naive' outer expansion (32) immediately shows the propagation speed to be $C_0 \equiv A/B = (n+1)(1-\epsilon_0)$. But we notice that C_0 was non-dimensionalized with respect to $U_0 = \epsilon_0^n U_{\mathrm{t}}$, which is a function of ϵ_0 itself. To remove this dependence, we introduce $\tilde{C}_0 \equiv C_0\epsilon_0^n$, which is again a function of the material properties of the bed alone. The propagation speed is now given by

$$\tilde{C}_0 = (n+1)\epsilon_0^n(1-\epsilon_0), \tag{45}$$

which is valid when t is $O(1)$. If we now define the propagation speed to be the rate of change of the position separating the exponential and oscillatory behaviour given by the uniformly valid outer expansion (37), the asymptotic propagation speed, as $t \to \infty$, is given by

$$\tilde{C} = \tilde{C}_0 - \frac{\{\tilde{P}_0 - \tilde{C}_0^2\}RF}{(n+1)\epsilon_0^{3n-1}}. \tag{46}$$

It should be noticed that (46) is essentially a corrected form of (45).

4. Numerical solution of the linearized problem

Solutions have been found in §3 to the linearized equations of motion for small Froude number. These solutions describe the propagation and evolution of a small-amplitude voidage disturbance through an otherwise uniformly fluidized bed. The evolution is shown to take place over three timescales. When t is $O(F)$ there is rapid adjustment in the amplitudes of the initial disturbances, which then propagate vertically upwards through the bed on a timescale $O(1)$, with dispersion and diffusion or 'instability' being felt on a timescale $O(F^{-1})$. If $\tilde{P}_0 > A^2/B^2$, then diffusion prevails, and asymptotic expansions, found as $t \to \infty$, show the disturbance to evolve into a

pulse followed by a wavetrain, the amplitudes decaying to zero as $t \to \infty$. On the other hand, if $\bar{P}_0 < A^2/B^2$, we have instability, with the amplitude of each wave component growing like $\exp(k^2F(A^2/B^2 - \bar{P}_0)\,t)$. This leads to the breakdown of the linearized theory, and hence of the validity of the linearized solution, on a timescale of $O(F^{-1})$.

To confirm the solutions obtained for small F, and compare the behaviour as F is increased to $O(1)$, the linearized equations (21), (17) and (18) will be solved numerically subject to initial and boundary conditions (20). Equation (21) for $\bar{E}$ is solved using an implicit Crank–Nicolson finite-difference scheme, $\bar{V}$ is then calculated from (18) via integration using the trapezium rule. It is then straightforward to determine $\bar{U}$ from the algebraic equation (17). For the numerical solution, the form of the initial disturbance $g(x)$ was taken to be $\exp(-x^2)$. Step lengths 0.05 in the x-direction and 0.01 in the time direction were used throughout, with the boundary condition at $x \to \pm\infty$ applied at $x = \pm 40$.

To fix things, a typical case $F = 0.005$, $\epsilon_0 = 0.4$, $R = 1.0$ was chosen, and solutions have been calculated for this typical case and for varying F, ϵ_0 and R about this. Four cases are shown graphically in figures 2(*a–e*), where graphs of $\bar{E}$ are plotted against x for varying times. Qualitative agreement with the analytical solution is clear. In all of the cases computed, propagation, dispersion and diffusion or instability are apparent, and take effect on the timescales confirmed by the analytical solutions. The numerical results also confirm that the propagation speed is affected to leading order only by changes in ϵ_0; changes in R and $\bar{P}_0$ introduce only small corrections. Numerically, we find the propagation speed decreases with increasing F, decreases with increasing ϵ_0 (when scaled with U_0) and increases with increasing R. We also notice that for a given, stable, flow rate with corresponding uniform voidage ϵ_0, diffusion becomes greater with increasing F, and dispersion more apparent with decreasing R.

5. The nonlinear problem

The linearized theory examined the evolution of small-amplitude disturbances in voidage made to an initially uniformly fluidized state. It was found that, depending upon the flow rate, and hence the voidage ϵ_0, of the uniform state, the amplitude of the disturbance would either decay or grow exponentially on a timescale $O(F^{-1})$. Although the linearized theory has enabled us to predict the flow rates at which the uniform state can exist (i.e. is stable) under small-amplitude disturbances, and maybe even tentatively suggest, by comparison with experimental results of Zenz & Othmer (1960), that when the flow rate is such that the uniform state is unstable slugging may develop, to study such phenomena further nonlinear effects must be considered.

To study nonlinear effects, the initial-value problem is examined for finite-amplitude disturbances governed by the nonlinear equations (11)–(13). Here we find that a more convenient velocity scale with which to non-dimensionalize is U_t, the terminal free-fall velocity of a particle, where $U_0 = U_t \epsilon_0^n$. After non-dimensionalizing with U_t, (11)–(13) become

$$EU + (1-E)\,V = \tilde{M}_0, \tag{47a}$$

$$-\frac{\partial E}{\partial t} + \frac{\partial}{\partial x}\{(1-E)\,V\} = 0, \tag{47b}$$

$$\tilde{F}(1-E)\left\{\frac{\partial V}{\partial t} + V\frac{\partial V}{\partial x}\right\} = \tilde{B}(E)\,(U-V) - (1-E) + \tilde{F}\tilde{P}_0\frac{\partial E}{\partial x} + \frac{\tilde{F}}{\tilde{R}}\frac{\partial^2 V}{\partial x^2}, \tag{47c}$$

where $\tilde{B}(E) = (1-E)/E^n$, $\tilde{F} = U_t^2/gh$ and $\tilde{R} = \rho_s U_t h/\bar{\mu}_s$, and again we have

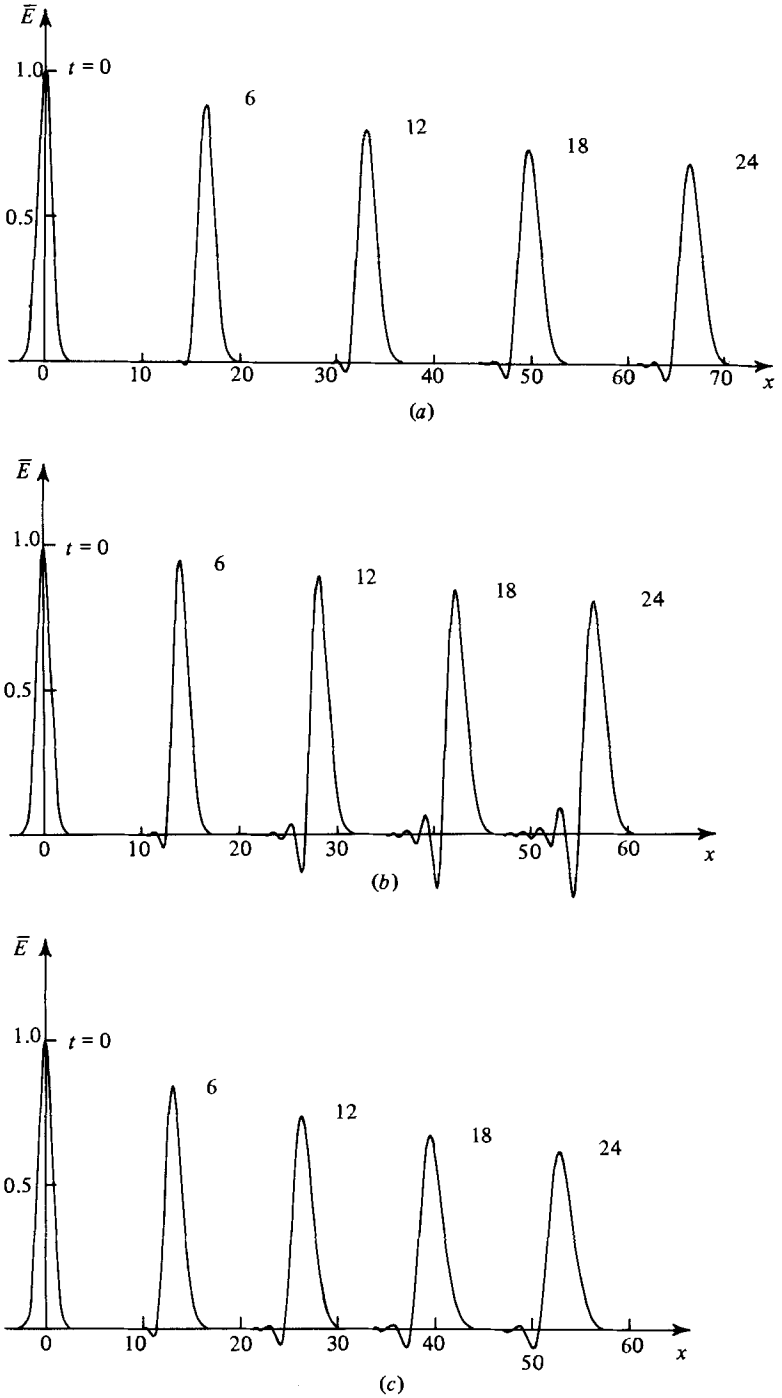

FIGURE 2(*a–c*). For caption see facing page.

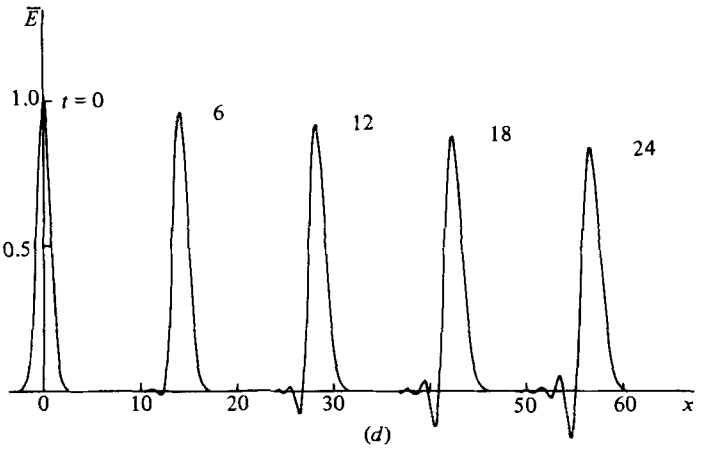

FIGURE 2. Voidage perturbation $\bar{E}$ against x up to $t = 24$ when: (*a*) $\epsilon_0 = 0.3$, $F = 0.005$, $R = 1.0$, $\bar{P}_0 = 0.05$, $n = 3$; (*b*) $\epsilon_0 = 0.4$, $F = 0.005$, $R = 0.25$, $\bar{P}_0 = 0.05$, $n = 3$; (*c*) $\epsilon_0 = 0.4$, $F = 0.04$, $R = 1.0$, $\bar{P}_0 = 0.05$, $n = 3$; (*d*) $\epsilon_0 = 0.4$, $F = 0.005$, $R = 1.0$, $\bar{P}_0 = 0.05$, $n = 3$.

$\tilde{F} = F\epsilon_0^{-2n} \ll 1$. The initial conditions are given by (14) and (15), and far away from the disturbance we have $E \to \epsilon_0$, $V \to 0$ and $U \to \epsilon_0^n$. Also since $0 \leqslant E \leqslant 1$ for all times, the initial amplitude must satisfy $\alpha \leqslant 1 - \epsilon_0$. A further restriction $\alpha \geqslant 0$ is made as we are interested in the propagation of high-voidage regions only, although cases for which $\alpha < 0$ can be studied in a similar manner. $\tilde{M}_0$ is the total volume flow, and, applying the conditions far away from the disturbance, we find $\tilde{M}_0 = \epsilon_0^{n+1}$.

Using (47*a*), we eliminate U from (47*c*), which becomes, after substitution for $\tilde{B}(E)$,

$$\tilde{F}(1-E)\left\{\frac{\partial V}{\partial t} + V\frac{\partial V}{\partial x}\right\} = \frac{(1-E)(\tilde{M}_0 - V)}{E^{n+1}} - (1-E) + \tilde{F}\tilde{P}_0\frac{\partial E}{\partial x} + \frac{\tilde{F}}{\tilde{R}}\frac{\partial^2 V}{\partial x^2}. \tag{48}$$

Equations (47*b*) and (48) are two equations for E and V. We now obtain a single equation for the voidage E by neglecting terms $O(\tilde{F}^2)$. Since $E \not\equiv 1$, (48) gives

$$V = \tilde{M}_0 - E^{n+1} + O(\tilde{F}). \tag{49}$$

V is now replaced in (48) by (49) in all but leading-order terms, which leads to

$$V = \tilde{M}_0 - E^{n+1} + \tilde{F}\phi(E, E_x, E_t, E_{xx}, \tilde{M}_0) + O(\tilde{F}^2), \tag{50}$$

where

$$\phi = (n+1)E^{2n+1}\left\{\frac{\partial E}{\partial t} + (\tilde{M}_0 - E^{n+1} + \tilde{P}_0((1-E)(n+1)E^n)^{-1}\frac{\partial E}{\partial x} - \frac{E^{n+1}}{\tilde{R}(1-E)}\frac{\partial^2}{\partial x^2}(\tilde{M}_0 - E^{n+1})\right\}.$$

Substituting (50) for V into (47*b*), we have on re-arrangement

$$\frac{\partial E}{\partial t} + \{\tilde{M}_0 + (n+1)E^n - (n+2)E^{n+1}\}\frac{\partial E}{\partial x} = \tilde{F}\frac{\partial}{\partial x}\{(1-E)\phi\} + O(\tilde{F}^2), \tag{51}$$

and to leading order

$$\frac{\partial}{\partial t} \approx -\{\tilde{M}_0 + (n+1)E^n - (n+2)E^{n+1}\}\frac{\partial}{\partial x}. \tag{52}$$

Equation (52) is now used to replace $\partial/\partial t$ in ϕ. Finally, substitution of ϕ into (51)

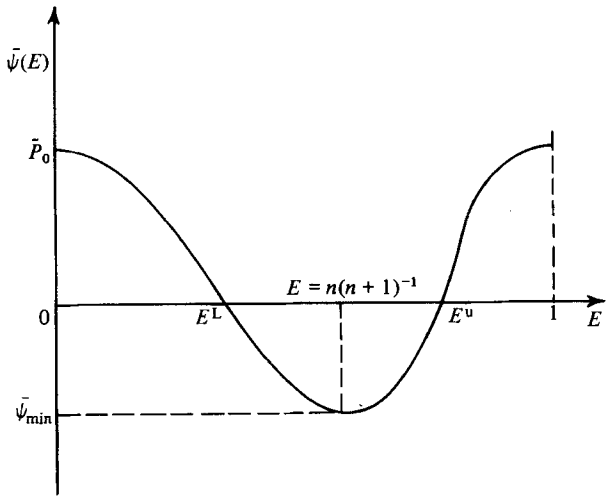

FIGURE 3. A graph of $\bar{\psi}(E)$ against E.

and neglecting terms of $O(\tilde{F}^2)$ leads to a single equation for voidage, namely

$$\frac{\partial E}{\partial t}+C(E)\frac{\partial E}{\partial x}=\tilde{F}\frac{\partial}{\partial x}\left\{\psi(E)\frac{\partial E}{\partial x}+\frac{E^{n+1}}{\tilde{R}}\frac{\partial^2\eta(E)}{\partial x^2}\right\}, \tag{53}$$

where

$$C(E)=\tilde{M}_0+(n+1)E^n-(n+2)E^{n+1}, \tag{54}$$

$$\psi(E)=E^{n+1}\{\tilde{P}_0-(n+1)^2(1-E)^2E^{2n}\}=E^{n+1}\bar{\psi}(E), \tag{55}$$

$$\eta(E)=\tilde{M}_0-E^{n+1}. \tag{56}$$

The left-hand side represents nonlinear convection, while the $O(\tilde{F})$ terms on the right-hand side represent nonlinear diffusion and dispersion, although the effect of dispersion is expected to be weak for $\tilde{R}=O(10)$. To leading order, we expect propagation determined by the left-hand side, the right-hand side being negligible except in regions where $\partial^2E/\partial x^2$ is $O(F^{-1})$. In such regions we expect 'local diffusion' if $\psi(E)>0$, but 'local concentrating' of voidage if $\psi(E)<0$. Examination of $\bar{\psi}(E)$ for $0<E<1$ shows it to have one minimum at $E=n(n+1)^{-1}$ and two roots at E^{L} and E^{u} provided that $0<\tilde{P}_0<(n(n+1))^{2n}$, which is expected physically. This can be seen in figure 3, where $\bar{\psi}(E)$ is plotted against E for $0<E<1$. Thus it is immediately clear that the exponential growth of a disturbance made to an unstable uniform state (i.e. $E^{\mathrm{L}}<\epsilon_0<E^{\mathrm{u}}$), as predicted by the linearized theory, is curbed by the nonlinearity of the diffusion coefficient $\psi(E)$ in (53), owing to the change in sign at E^{u} and E^{L}. It should also be noted, for alternative choices of $P_{\mathrm{s}}(E)$, that $\psi(E)$ always has at most two zeros, provided only that $P_{\mathrm{s}}(E)$ is a monotonically decreasing function of E and that $P_{\mathrm{s}}(E)\to 0$ as $E\to 1$.

The solution of the initial-value problem is now determined using equations (53), (50) and (47a) for E, V and U respectively. In deriving these equations, we notice that, as with the linearized problem, a time derivative has been lost, namely $\partial V/\partial t$, enabling only one of the initial conditions (14) and (15) to be satisfied. Consequently, as with the linearized problem, an inner region of the same time scaling must be considered first to determine the appropriate initial condition to be applied to the outer equations (53), (50) and (47a). Solution of the inner problem determines the

inner expansions, in terms of the inner variable $\bar{t}$, as

$$E_{\mathrm{I}}(x,\bar{t}) = \epsilon_0+\alpha g(x)+O(\tilde{F}),$$

$$V_{\mathrm{I}}(x,\bar{t}) = \{\tilde{M}_0-(\epsilon_0+\alpha g(x))^{n+1}\}\{1-\exp(-\bar{t}(\epsilon_0+\alpha g(x))^{-(n+1)})\}+O(\tilde{F}),$$

$$U_{\mathrm{I}}(x,\bar{t}) = \{\tilde{M}_0-(1-\epsilon_0-\alpha g(x))(\tilde{M}_0-(\epsilon_0+\alpha g(x))^{n+1}) \times(1-\exp\{-\bar{t}(\epsilon_0+\alpha g(x))^{-(n+1)}\})\}(\epsilon_0+\alpha g(x))^{-1}+O(\tilde{F}),$$

showing that the appropriate initial condition for E to be applied to (53) is $E(x,0) = \epsilon_0+\alpha g(x)$. First we solve the leading-order problem, neglecting terms on the right-hand side of (53). The problem then reduces to solving the equation

$$\frac{\partial E}{\partial t}+C(E)\frac{\partial E}{\partial x} = 0 \tag{57}$$

subject to the initial condition (14), where $g(x)$ is taken as a 'single hump'. This is done, following Whitham (1974), using the method of characteristics. The solution is given implicitly by

$$E = \epsilon_0+\alpha g(s) \tag{58}$$

on the curves

$$x(t) = C(\epsilon_0+\alpha g(s))\,t+s \tag{59}$$

for all real values of the parameter s. Before proceeding to discuss the solution in detail, it is instructive to consider the functional form of $C(E)$. By considering $\mathrm{d}C/\mathrm{d}E$ and $\mathrm{d}^2C/\mathrm{d}E^2$ for $0 \leqslant E \leqslant 1$, C is found to have just one maximum at $E = n(n+2)^{-1}$; and a point of inflexion or local minimum at $E = 0$, according to whether n is odd or even. $C(E)$ is shown graphically in figure 4. Three distinct cases immediately arise, on examining the characteristic curves given by (59). First, if $\epsilon_0+\alpha \leqslant n(n+2)^{-1}$, then $C(E)$ is a monotonically increasing function for $\epsilon_0 \leqslant E \leqslant \epsilon_0+\alpha$, so the higher values of E propagate with faster speeds, causing the 'single hump' to break at the front and become multivalued after a certain time. On the other hand, if $\epsilon_0 \geqslant n(n+2)^{-1}$, then $\epsilon_0+\alpha > n(n+2)^{-1}$, and $C(E)$ is a monotonically decreasing function of E for $\epsilon_0 \leqslant E \leqslant \epsilon_0+\alpha$; therefore lower values of E propagate with higher speeds, causing the 'single hump' to break at the back. The third case occurs when $\epsilon_0 < n(n+2)^{-1}$ and $\epsilon_0+\alpha > n(n+2)^{-1}$; since $C(E)$ has a local maximum at $E = n(n+2)^{-1}$, then after a certain time the 'single hump' becomes multivalued at both 'back' and 'front'.

When the solution becomes multivalued, we infer that some assumption in the derivation of (57) has been violated (namely the neglect of higher-order terms on the right-hand side of (53)).

To proceed further we must allow discontinuous solutions (the structures of which will be examined later) as follows. Equation (57) comes directly from the particle-phase continuity equation (46), which is a statement of conservation of mass in the particle phase, assuming the continuity and differentiability of $V(x,t)$ and $E(x,t)$. Relaxing the assumption of differentiability, the conservation law may be stated in integral form as

$$-\frac{\partial}{\partial t}\int_{x_1}^{x_2} E(x,t)\,\mathrm{d}x+[(1-E)\,V]_{x_1}^{x_2} = 0. \tag{60}$$

With V given by the lower-order approximation (49), we now follow Whitham (1974) in replacing multivalued solutions of (57) by the appropriate discontinuous solutions of (60). Whitham shows that this is equivalent to fitting a discontinuity into the multivalued solution of (60) which satisfies the two conditions that the discontinuity must remove the multivalued regions and that the areas under the discontinuous curve and the multivalued curve must be equal.

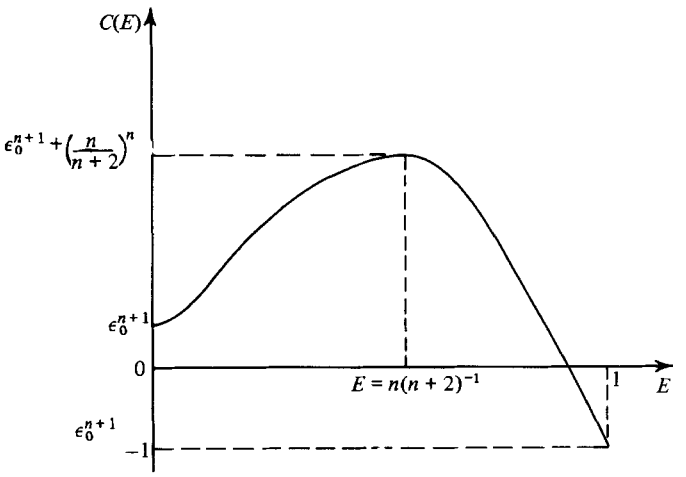

FIGURE 4. A graph of $C(E)$ against E.

We have shown so far that continuous 'single-hump' initial conditions will always become discontinuous in finite time, either at front, back, or both, depending upon the uniform voidage ϵ_0 and the amplitude α of the initial disturbance. The solution is now found in more detail. To fix things, $g(x)$ is taken as

$$g(x) = \begin{cases} 1-x^2 & (|x| \leqslant 1), \\ 0 & \text{(elsewhere)}, \end{cases}$$

although it is shown later that the asymptotic behaviour as $t \to \infty$ is dependent only upon the value of $\int_{-\infty}^{\infty} g(x)\,dx$ when $g(x)$ is a single hump. Using (58) and (59), the solution is

$$E = \begin{cases} \epsilon_0+\alpha(1-s^2) & (|s| \leqslant 1), \\ \epsilon_0 & (|s| > 1) \end{cases} \tag{61a}$$

on the curves

$$x(s,t) = \begin{cases} C(\epsilon_0+\alpha(1-s^2))\,t+s & (|s| \leqslant 1), \\ (n+1)\,\epsilon_0^n(1-\epsilon_0)\,t+s & (|s| > 1). \end{cases} \tag{61b}$$

The solution defined by (60) and (61) first becomes multivalued at a time t_B given by

$$t_B^{-1} = -\{C(f(s))_{\max}; -\infty < s < \infty\}, \quad \text{where} f(s) = \epsilon_0+\alpha(1-s^2).$$

On examining $C(f(s))'$ we find that $t_B > 0$ for all $0 < \epsilon_0 < 1$ and $\alpha > 0$. Further examination of the characteristic s_B on which breakdown first occurs confirms the three cases previously mentioned. These cases are now considered in turn.

(i) $\epsilon_0+\alpha \leqslant n(n+2)^{-1}$

The solution given by (61) becomes multivalued for $t > t_B$. To obtain an expression for t_B explicitly involves solving a fourth-order polynomial, which has to be done numerically, although we can find an upper bound, which is given by

$$0 \leqslant t_B \leqslant \{2\alpha(n+1)\,\epsilon_0^{n-1}(n-(n+2)\,\epsilon_0)\}^{-1}.$$

The compressive region is bounded by the characteristics $s = 1$ and $s = 0$, and for $t > t_B$ a single-valued solution is recovered by fitting a discontinuity at $x = l(t)$, as shown in figure 5, where $H(t)$ and $h(t)$ are the values of E directly behind and ahead

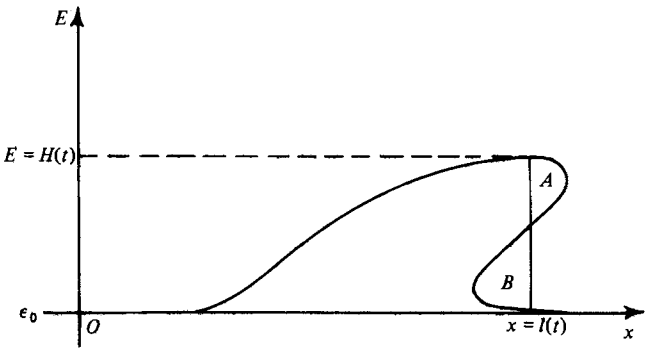

FIGURE 5. The multivalued solution of case (i).

of the discontinuity respectively. The discontinuity is fitted such that

$$\text{area } (A) = \text{area } (B). \tag{62}$$

Returning to (60) and (61) giving $E = E(s)$ on $x = x(t, s)$, inversion of (61*a*) for $|s| \leqslant 1$ gives

$$s = \pm\{(\epsilon_0 + \alpha - E)\,\alpha^{-1}\}^{\frac{1}{2}} \tag{63}$$

and substitution of (63) into (61*b*) gives

$$x(E, t) = C(E)\,t \pm \{(\epsilon_0 + \alpha - E)\,\alpha^{-1}\}^{\frac{1}{2}} \tag{64}$$

(taking the positive or negative sign according to whether s is positive or negative on the characteristic in consideration). For characteristics on which s is positive we define $x(t, E) \equiv x^+(t, E)$, and, for characteristics on which s is negative, $x(t, E) \equiv x^-(t, e)$. Using this notation, (62) becomes

$$(H(t) - h(t))\,l(t) = \int_{h(t)}^{\epsilon_0 + \alpha} x^+(t, E)\,\mathrm{d}E - \int_{H(t)}^{\epsilon_0 + \alpha} x^-(t, E)\,\mathrm{d}E, \tag{65}$$

and from (64) we have

$$l(t) = C(H(t))\,t - \{(\epsilon_0 + \alpha - H(t))\,\alpha^{-1}\}^{\frac{1}{2}}, \tag{66}$$

$$l(t) = C(h(t))\,t + (\epsilon_0 + \alpha - h(t))\,\alpha^{-1}\}^{\frac{1}{2}}. \tag{67}$$

Relations (65)–(67) are three equations for the three unknowns $l(t), h(t), H(t)$. But we notice that in this case the discontinuity always moves into the undisturbed region, so that $h(t) \equiv \epsilon_0$, and the characteristics meeting the front of the discontinuity have $s > 1$. Thus we must replace (67) by

$$l(t) = C(\epsilon_0)\,t + s. \tag{68}$$

Substituting $h(t) = \epsilon_0$ into (65) and (66) gives two equations for $H(t)$ and $l(t)$; (68) then determines the value of s on the characteristic ahead of the discontinuity. If x^+ and x^- are now substituted from (64) into (65), this on integration, after replacing $l(t)$ by (66), gives a single algebraic equation for $H(t)$, namely

$$\begin{aligned}(n+1)\,H^{n+2} - \{n + (n+2)\,\epsilon_0\}\,H^{n+1} + (n+1)\,\epsilon_0 H^n - \epsilon_0^{n+1}(1-\epsilon_0) \\ + \{(H-\epsilon_0)\,\{(\epsilon_0 + \alpha - H)\,\alpha^{-1}\}^{\frac{1}{2}} + \tfrac{2}{3}\alpha + \tfrac{2}{3}\alpha\{(\epsilon_0 + \alpha - H)\,\alpha^{-1}\}^{\frac{3}{2}}\}\,t^{-1} = 0.\end{aligned} \tag{69}$$

Equation (69) can be solved asymptotically for large t; we find

$$H(t) = \epsilon_0 + \left\{\frac{8\alpha}{3(n+1)\,(n-(n+2)\,\epsilon_0)}\right\}^{\frac{1}{2}} t^{-\frac{1}{2}} + O(t^{-1}). \tag{70}$$

Equation (66) is now used to determine $l(t)$ as $t \to \infty$, namely

$$l(t) = (n+1)\,\epsilon_0^n(1-\epsilon_0)\,t + 2\epsilon_0^{n-1}\{\tfrac{2}{3}\alpha(n+1)\,(n-(n+2)\,\epsilon_0)\}^{\frac{1}{2}}\,t^{\frac{1}{2}} + O(1). \tag{71}$$

The solution behind the discontinuity is given by (60) and (61), and takes the asymptotic form

$$E(x,t) = \begin{cases} \epsilon_0 + \dfrac{x-\epsilon_0^n(n+1)\,(1-\epsilon_0)\,t}{\epsilon_0^{n-1}(n+1)\,(n-(n+2)\,\epsilon_0)\,t} & ((n+1)\,\epsilon_0^n(1-\epsilon_0)\,t \leqslant x \leqslant l(t)), \\ \epsilon_0 \quad \text{(elsewhere)}. \end{cases}$$

Equations (69) and (66) have been solved numerically, using Newton's method to determine $H(t)$ and $l(t)$ for smaller times. It should be noted that (69) and (66) determining $H(t)$ and $l(t)$ are valid only for $t \geqslant t^*$, where t^* is the time at which $H(t) = \epsilon_0 + \alpha$, and is given by

$$t^* = 2\alpha\{\alpha C(\epsilon_0+\alpha) - \int_{\epsilon_0}^{\epsilon_0+\alpha} C(E)\,\mathrm{d}E\}^{-1}.$$

When $t_B \leqslant t \leqslant t^*$ the appropriate equations for $H(t)$ and $l(t)$ are

$$(H(t)-\epsilon_0)\,l(t) = \int_{\epsilon_0}^{H} x^+(E,t)\,\mathrm{d}E,$$

$$l(t) = C(H)\,t + \{(\epsilon_0+\alpha-H)\,\alpha^{-1}\}^{\frac{1}{2}}.$$

The numerical results are compared with the asymptotic solutions in figure 6, discontinuity height $H(t)$ being plotted against time t for the case $\epsilon_0 = 0.3$, $\alpha = 0.2$ and $n = 3.0$.

(ii) $\epsilon_0 \geqslant n(n+2)^{-1}$

In this case the compressive region is at the rear of the hump, bounded by the characteristics $s = -1$ and $s = 0$. As with (i), the solution becomes multivalued for $t > t_B$, where t_B now satisfies the inequality

$$0 \leqslant t_B \leqslant \{2\alpha(n+1)\,\epsilon_0^{n-1}((n+2)\,\epsilon_0 - n)\}^{-1}.$$

Following the methods described in the previous case, we find the asymptotic forms for discontinuity height $H(t)$ and position $l(t)$ as $t \to \infty$ are given by

$$H(t) = \epsilon_0 + \left\{\frac{8\alpha}{3(n+1)\,((n+2)\,\epsilon_0 - n)}\right\}^{\frac{1}{2}} t^{-\frac{1}{2}} + O(t^{-1}),$$

$$l(t) = (n+1)\,\epsilon_0^n(1-\epsilon_0)\,t - 2\epsilon_0^{n-1}\{\tfrac{2}{3}\alpha(n+1)\,((n+2)\,\epsilon_0 - n)\}^{\frac{1}{2}}\,t^{\frac{1}{2}} + O(1),$$

$$E(x,t) = \begin{cases} \epsilon_0 + \dfrac{\epsilon_0^n(1-\epsilon_0)\,(n+1)\,t - x}{\epsilon_0^{n-1}(n+1)\,((n+2)\,\epsilon_0 - n)\,t} & (l(t) \leqslant x \leqslant (n+1)\,\epsilon_0^n(1-\epsilon_0)\,t), \\ \epsilon_0 \quad \text{(elsewhere)}. \end{cases}$$

(iii) $\epsilon_0 < n(n+2)^{-1}$ *and* $(\epsilon_0+\alpha) > n(n+2)^{-1}$

For this case a detailed analysis is more complicated, although examination of the characteristic curves (61*b*) shows that there are compressive regions at both front and back. Thus after sufficient time the solution becomes multivalued at front and back. A single-valued solution is recovered by fitting the two appropriate discontinuities. The asymptotic behaviour is of a more complicated nature in this case, although it may be shown that eventually the two discontinuities merge at the front, after which further development is very similar to that of case (i).

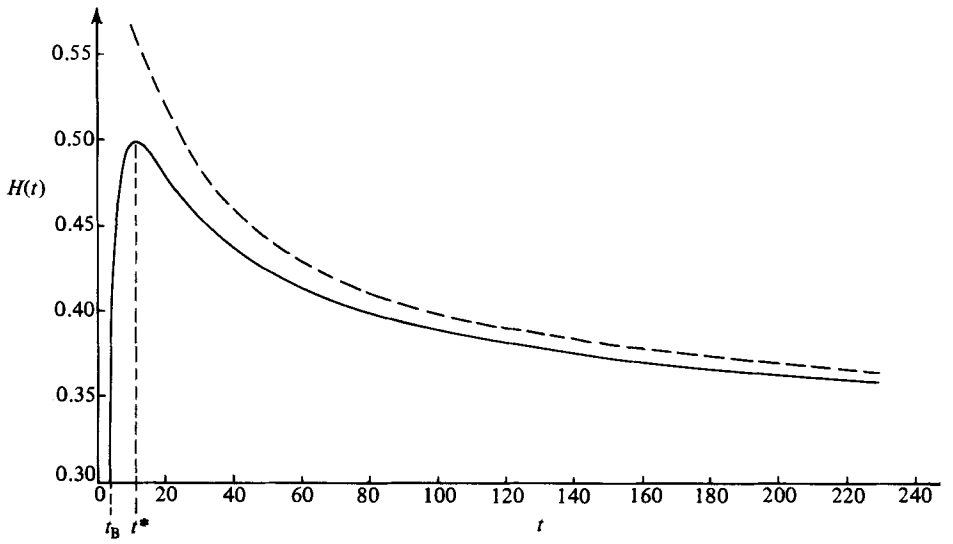

FIGURE 6. Graphs of discontinuity height $H(t)$ against time, as calculated from the numerical solution (solid line) and the asymptotic solution (broken line) when $\epsilon_0 = 0.3$, $\alpha = 0.2$ and $n = 3.0$.

By considering solutions to the lower-order approximation of (53) for $\tilde{F} \ll 1$, we have found that finite-amplitude disturbances made to the uniform state develop discontinuities, the details of which depend upon ϵ_0 and hence the flow rate of the uniform state, and the amplitude α of the initial disturbance. We expect the discontinuities in the lower-order approximation to occur due to the neglect of higher-order terms on the right-hand side of (58) in regions of rapid change. The structure of the lower-order discontinuities is now examined by introducing higher-order derivatives into such regions. By doing this we are able to assess the timescales upon which the lower-order approximations are valid.

6. Discontinuity structure

The structure of discontinuities arising in the solution of the lower-order approximation is now examined. We suppose the discontinuity is positioned at $x = l(t)$ and moving with speed $U = \dot{l}(t)$; ahead of the discontinuity $E = h(t)$ and behind $E = H(t)$. The coordinate y is introduced such that the discontinuity is at $y = 0$. y is defined by

$$y = x - \int_{t_B}^{t} U(w)\,\mathrm{d}w.$$

In terms of y and t, (53) becomes

$$\frac{\partial E}{\partial t} + \{C(E) - U\}\frac{\partial E}{\partial y} = \tilde{F}\frac{\partial}{\partial y}\left\{\psi(E)\frac{\partial E}{\partial y} + \frac{E^{n+1}}{\tilde{R}}\frac{\partial^2 \eta}{\partial y^2}\right\}. \tag{72}$$

Within a region about $y = 0$, we wish to introduce the higher-order terms on the right-hand side of (72) to leading order in $\tilde{F}$. To simplify, as a first approximation to the structure problem, we assume $\tilde{R} \gg 1$ and tentatively neglect the final term on the right-hand side of (72). The appropriate stretched variable is then found to be $Y = y\tilde{F}^{-1}$, (72) becoming, in terms of Y,

$$\tilde{F}\frac{\partial E}{\partial t} + \{C(E) - U\}\frac{\partial E}{\partial Y} = \frac{\partial}{\partial Y}\left\{\psi(E)\frac{\partial E}{\partial Y}\right\}. \tag{73}$$

Thus, on this scaling, to leading order the structure is quasisteady and is determined by the solution of

$$\frac{\partial}{\partial Y}\{Q(E)-UE\} = \frac{\partial}{\partial Y}\left\{\psi(E)\frac{\partial E}{\partial Y}\right\}, \tag{74}$$

where $Q(E) = \int_0^E C(E)\,\mathrm{d}E$ and the following conditions must be satisfied:

$$\left.\begin{aligned} E &\to H(t) \quad \text{as} \quad Y \to -\infty, \\ E &\to h(t) \quad \text{as} \quad Y \to +\infty. \end{aligned}\right\} \tag{75}$$

Equation (74) can be integrated once to give

$$\frac{\partial E}{\partial Y} = \frac{Q(E)-UE+A_0}{\psi(E)} \equiv G(E), \tag{76}$$

where A_0 is an arbitrary constant. We now consider in detail the existence of quasisteady structures for discontinuities arising in case (i) of the lower-order approximation. Thus we have $h(t) = \epsilon_0$ and $H(t) \leqslant \epsilon_0+\alpha \leqslant n(n+2)^{-1}$. Applying (75) gives

$$\left.\begin{aligned} U &= \{Q(H(t))-Q(\epsilon_0)\}\,\alpha^{-1}, \\ A_0 &= \{Q(H(t))\,\epsilon_0 - Q(\epsilon_0)\,H(t)\}\,\alpha^{-1}. \end{aligned}\right\} \tag{77}$$

We notice that the relation for U in (77) agrees with the discontinuity speed $l(t)$ for the lower-order approximation. We proceed to examine the right-hand side of (76) for $\epsilon_0 \leqslant E \leqslant \epsilon_0+\alpha$. First consider α such that $\epsilon_0+\alpha < E^{\mathrm{L}}$ (E^{L} is the smaller of the two roots of ψ for $0 \leqslant E \leqslant 1$), then $\psi(E)$ is positive for $\epsilon_0 \leqslant E \leqslant \epsilon_0+\alpha$. The numerator of G, $N(E) = Q(E)-UE+A_0$, has roots at ϵ_0 and $\epsilon_0+\alpha$, and stationary points when

$$N'(E) \equiv C(E)-U = 0. \tag{78}$$

But we also have the compatibility condition

$$C(H(t)) > U > C(\epsilon_0), \tag{79}$$

which must be satisfied for a discontinuity to exist in the lower-order approximation. Equation (78) and the inequality (79) show that $N(E)$ has at least one stationary point for $\epsilon_0 \leqslant E \leqslant H(t)$, but, since $C(E)$ is a monotonically increasing function on this range, then $N(E)$ has just one stationary point. Using (78) and (79) we have also that $N'(\epsilon_0) < 0$. Together these results show that $G(E) < 0$ for $\epsilon_0 < E < H(t)$. Thus, under these conditions, it is possible to fit a smooth, monotonic, integral curve of (76) satisfying the two end conditions (75).

We now examine discontinuities for which $E^{\mathrm{L}} \leqslant H(t) \leqslant n(n+2)^{-1}$. As before, the numerator $N(E)$ is always negative on the range $\epsilon_0 < E < H(t)$, but $\psi(E^{\mathrm{L}}) = 0$; thus $G(E)$ has a singularity at E^{L}. Clearly in this case there is no single-valued integral curve of (76) satisfying end conditions (75), and thus a quasisteady structure for such discontinuities is not possible.

Similarly, for discontinuities occurring in case (ii) of the lower-order problem, we find that a smooth monotonic integral curve of (76) satisfying the appropriate end conditions can be found only when $\epsilon_0 > E^{\mathrm{u}}$ (which implies $\epsilon_0+\alpha > E^{\mathrm{u}}$ as we are taking $\alpha > 0$). For case (iii), since we expect $E^{\mathrm{L}} < n(n+2)^{-1}$, $G(E)$ always has a singularity over the range considered, and again no quasisteady structure can be found.

Thus we find, when $\tilde{R} \gg 1$, that discontinuities arising in the solution of the lower-order problem can be smoothed out by considering higher-order terms over a

region of thickness $O(\tilde{F})$ provided that one of two conditions is satisfied by the initial amplitude and uniform voidage, namely

$$\epsilon_0+\alpha < E^{\mathrm{L}} \quad \text{or} \quad \epsilon_0 > E^{\mathrm{u}}. \tag{80}$$

That is, the uniform state must be stable according to the linearized theory, and the initial amplitude of the disturbance not between or on the critical values E^{L} and E^{u}. When this is so, we expect the solution of the lower-order approximation, augmented by the structure when y is $O(\tilde{F})$, to give a valid approximation to the full solution of (58). For small times, the term $\tilde{F}\,\partial E/\partial t$ in (73) must be included to leading order in the transition period when the steepening of the initial disturbance due to nonlinear convection becomes balanced by diffusion, resulting in the quasi-steady structure when $t = O(1)$.

It should be noted at this stage that, for beds in which $\psi(E) > 0$ for all $0 < E < 1$ (i.e. $\tilde{P}_0 > \{(1-E)^2 E^{2n}(n+1)^2\}_{\max}$, and are thus stable according to the linearized theory at all flow rates), the roots E^{L} and E^{u} are complex, and the structure for the lower-order discontinuities can be found for all ϵ_0 and $\epsilon_0+\alpha$. For such beds the lower-order solution augmented by the structure gives a valid approximation for all finite-amplitude disturbances made to uniform states at any flow rate. Since this is rare in most gas-fluidized beds, we now restrict attention to beds for which $\tilde{P}_0 \leqslant \{(1-E)^2 E^{2n}(n+1)^2\}_{\max}$ and hence $0 < E^{\mathrm{L}} \leqslant E^{\mathrm{u}} < 1$.

If neither of the conditions (80) is satisfied we have shown that it is not possible to smooth out lower-order discontinuities by introducing a quasisteady structure satisfying (76). This is due to a singularity in the structure equation (76) at the critical values E^{L} and E^{u}. The singularity arises since we have neglected the term $(\partial/\partial y)\,(E^{n+1}/\tilde{R}\,\partial^2\eta/\partial y^2)$ in deriving the structure equation (76) on the approximation $\tilde{R} \gg 1$. This is now seen to be a valid approximation provided that E nowhere lies in the neighbourhood of, or between, the critical values E^{L} and E^{u}. This becomes immediately clear on examining the full equation (72). When E lies away from E^{L} or E^{u}, then the structure is found by a balance between the left-hand side and the first term on the right-hand side of (72) for $\tilde{R} \gg 1$, but, if E lies close to E^{L} or E^{u} in any neighbourhood throughout the structure, then, no matter how large $\tilde{R}$, there is always a region about the critical point in which the balance determining the structure 'switches' to a balance between the left-hand side and the final term on the right-hand side, since in this region $\psi(E)$ becomes arbitrarily small.

It now remains to determine the behaviour of the bed when the flow rate is such that the uniform state is unstable, that is $E^{\mathrm{L}} < \epsilon_0 < E^{\mathrm{u}}$, and to determine the behaviour of finite-amplitude disturbances made to a stable uniform state, when the initial amplitude $\epsilon_0+\alpha$ approaches one of the critical values E^{L} or E^{u}.

We consider a simpler problem which enables the second question to be answered and indicates the behaviour sought in the first. Attention is limited to the propagation of a plane voidage front governed by (53) subject to the step initial conditions

$$E(x,0) = \begin{cases} \epsilon_0+\alpha & (x<0), \\ \epsilon_0 & (x>0), \end{cases} \tag{81}$$

which can be related to the physically definable problem of increasing the flow rate of an initially uniformly fluidized bed. We restrict $\epsilon_0 < E^{\mathrm{L}}$, so that the uniform state is stable according to the linearized theory (the case $\epsilon_0 > E^{\mathrm{u}}$ could also be considered in a similar manner), and consider the behaviour as the initial 'amplitude' $\epsilon_0+\alpha$ approaches and passes through the critical point E^{L}. The solution of the lower-order

problem, subject to initial conditions (81), is readily given by

$$E(x,t) = \begin{cases} \epsilon_0+\alpha & (x < Ut), \\ \epsilon_0 & (x > Ut), \end{cases} \tag{82}$$

where $U = \{Q(\epsilon_0+\alpha)-Q(\epsilon_0)\}\alpha^{-1}$. This is just a discontinuity propagating vertically upwards with speed U, ahead of which $E = \epsilon_0$, while behind $E = \epsilon_0+\alpha$. As before, we expect the higher-order terms on the right-hand side of (53) to be significant in a region close to the discontinuity. To determine the effect of these terms and the lengthscale of the region over which they are important for times of $O(1)$, we introduce the coordinate $y = x-Ut$ and examine quasisteady solutions of (53) that satisfy the end conditions $E \to \epsilon_0+\alpha$ as $y \to -\infty$ and $E \to \epsilon_0$ as $y \to \infty$. Introducing y into (53) shows, after integration and rearrangement, that quasisteady solutions must satisfy the equation

$$\tilde{F}\frac{\mathrm{d}^2E}{\mathrm{d}y^2}+\frac{n\tilde{F}}{E}\left(\frac{\mathrm{d}E}{\mathrm{d}y}\right)^2-\frac{\tilde{F}\tilde{R}\psi(E)}{(n+1)E^{2n+1}}\frac{\mathrm{d}E}{\mathrm{d}y}+\frac{\tilde{R}\{Q(E)-UE-A_0\}}{(n+1)E^{2n+1}} = 0, \tag{83}$$

where $A_0 = Q(\epsilon_0)-\{Q(\epsilon_0+\alpha)-Q(\epsilon_0)\}\epsilon_0\alpha^{-1}$. We proceed by studying the behaviour of solutions of (83) in the phase plane. Introducing $w = \mathrm{d}E/\mathrm{d}y$, (83) is rewritten as a pair of first-order equations

$$\left.\begin{aligned} \frac{\mathrm{d}E}{\mathrm{d}y} &= w \equiv G_1(E,w), \\ \frac{\mathrm{d}w}{\mathrm{d}y} &= \frac{\tilde{R}\psi(E)w}{(n+1)E^{2n+1}}-\frac{nw^2}{E}-\frac{\tilde{E}\{Q(E)-UE-A_0\}}{\tilde{F}(n+1)E^{2n+1}} \equiv G_2(E,w). \end{aligned}\right\} \tag{84}$$

The equilibrium points, which are solutions of $G_1(E,w) = G_2(E,w) = 0$, are at $E = \epsilon_0$ and $w = 0$; $E = \epsilon_0+\alpha$ and $w = 0$ and $E = \bar{\epsilon}(\epsilon_0,\alpha)$, $w = 0$, where $\bar{\epsilon}(\epsilon_0,\alpha) > \epsilon_0+\alpha > \epsilon_0$. We are concerned with paths in phase space (E,w) starting at $(\epsilon_0+\alpha,0)$ and terminating at $(\epsilon_0,0)$. To examine the existence and behaviour of such paths, the equilibrium points are firstly classified by their linearized approximations. The equilibrium point $(\epsilon_0,0)$ is found to be a saddle point, and in the neighbourhood of this point the appropriate behaviour is given by

$$E \sim \epsilon_0+B_0\exp\left(\left\{\frac{\tilde{R}\psi_0}{2(n+1)\epsilon_0^{2n+1}}-\frac{1}{2}\left[\frac{\tilde{R}^2\psi_0^2}{(n+1)^2\epsilon_0^{2(2n+1)}}+\frac{4\tilde{R}(U-C_0)}{\tilde{F}(n+1)\epsilon_0^{2n+1}}\right]^{\frac{1}{2}}\right\}y\right), \tag{85}$$

where B_0 is an arbitrary constant and $\psi_0 = \psi(\epsilon_0)$, $C_0 = C(\epsilon_0)$. In the neighbourhood of the equilibrium point $(\epsilon_0+\alpha,0)$, we find

$$E \sim (\epsilon_0+\alpha)+A_1\mathrm{e}^{\lambda_1 y}+A_2\mathrm{e}^{\lambda_2 y}, \tag{86}$$

where

$$\lambda_{1,2} = \frac{\tilde{R}\psi_\alpha}{2(n+1)(\epsilon_0+\alpha)^{2n+1}} \pm \frac{1}{2}\left\{\frac{\tilde{R}^2\psi_\alpha^2}{(n+1)^2(\epsilon_0+\alpha)^{4n+2}}-\frac{4\tilde{R}(C_\alpha-U)}{\tilde{F}(n+1)(\epsilon_0+\alpha)^{2n+1}}\right\}^{\frac{1}{2}}, \tag{87}$$

A_1, A_2 are arbitrary constants, $\psi_\alpha = \psi(\epsilon_0+\alpha)$ and $C_\alpha = C(\epsilon_0+\alpha)$. Thus, from (87), the equilibrium point $(\epsilon_0+\alpha,0)$ is a node provided that

$$\frac{\psi_\alpha^2\tilde{F}\tilde{R}}{4(n+1)(\epsilon_0+\alpha)^{2n+1}(C_\alpha-U)} \geqslant 1. \tag{88}$$

Otherwise it is a spiral, becoming a centre when $\psi_\alpha = 0$. Fixing $\epsilon_0 < E^{\mathrm{L}}$ and considering α in the range $\epsilon_0 < \epsilon_0+\alpha < E^{\mathrm{L}}$, we find that there is always a neighbourhood about ϵ_0, such that, when $\epsilon_0+\alpha$ lies in this neighbourhood, the inequality (88)

is satisfied. When this is so, the equilibrium point $(\epsilon_0+\alpha, 0)$ is a node, and by using the method of isoclines we find there is a path in phase space between the equilibrium points $(\epsilon_0+\alpha, 0)$ and $(\epsilon_0, 0)$. In this case the transition from $E = \epsilon_0$ ahead to $E = \epsilon_0+\alpha$ behind is monotonic.

Increasing α further, since $\psi_\alpha \to 0$ as $\epsilon_0+\alpha \to E^{\mathrm{L}}$, we find there is always a neighbourhood about E^{L} in which the inequality (88) is violated and the equilibrium point $(\epsilon_0+\alpha, 0)$ becomes a spiral point, paths spiralling out from $(\epsilon_0+\alpha, 0)$ in a clockwise sense. Again a path between the two equilibrium points exists. In this case oscillations appear on the downward side which are damped out as $y \to -\infty$, E approaching the constant value $\epsilon_0+\alpha$, while ahead, as before, E approaches the constant value ϵ_0 monotonically, as given by (85). We now use (85)–(87) to estimate the lengthscales over which $E \to \epsilon_0$ and $E \to \epsilon_0+\alpha$ ahead and behind, respectively, when $\tilde{F} \ll 1$. When $\tilde{R}$ is $O(1)$, the lengthscale over which $E \to \epsilon_0$ ahead is $O(\tilde{F}^{\frac{1}{2}}/\tilde{R}^{\frac{1}{2}})$, while behind the oscillations are damped out on a lengthscale $O(1/\tilde{R}\psi_\alpha)$.

More generally, for larger Reynolds numbers, when $\tilde{R}$ is $O(\tilde{F}^{-\delta})$ with $\delta \geqslant 1$, the lengthscale over which $E \to \epsilon_0$ is $O(\tilde{F})$, and the lengthscale over which the oscillations are damped out is now $O(\tilde{F}^{\delta}/\psi_\alpha)$. Thus, for $\epsilon_0+\alpha < E^{\mathrm{L}}$, as α is increased, the lengthscale over which the oscillations are damped also increases, since $\psi_\alpha \to 0$ as $\epsilon_0+\alpha \to E^{\mathrm{L}}$. Finally, when $\epsilon_0+\alpha = E^{\mathrm{L}}$, the equilibrium point $(\epsilon_0+\alpha, 0)$ becomes a centre, and with further increase in α becomes a spiral, with paths spiralling towards $(\epsilon_0+\alpha, 0)$ in a clockwise sense. Under these conditions a simple application of the Hopf bifurcation theorem shows that a limit cycle bifurcates from the equilibrium point $(\epsilon_0+\alpha, 0)$ as it passes through E^{L}. The path from $(\epsilon_0, 0)$ will not now reach $(\epsilon_0+\alpha, 0)$, but wind around the limit cycle; thus the oscillations will no longer be damped out, but persist as $y \to -\infty$.

Interpreting these results with regard to turning up the volume flow of a uniformly fluidized bed, suggests that for sufficiently small increases a plane front propagates upwards through the bed, separating the two regions of uniform voidage by a thin monotonic transition region. For larger increases, as $\epsilon_0+\alpha \to E^{\mathrm{L}}$, oscillations appear behind the transition region, which are damped out on a lengthscale $O(1/\tilde{R}\psi_\alpha)$. As $\epsilon_0+\alpha$ passes through E^{L} (ψ_α passes through zero), the oscillations are no longer damped and the state behind the transition region becomes oscillatory. This suggests that, when the uniform state is unstable according to the linearized theory, there is another, quasisteady, oscillatory state which the bed assumes. This is suggestive of a transition to slug flow, which appears as a quasisteady periodic state of the system, and shows great stability. The existence and temporal stability of a quasisteady periodic state of the full nonlinear equations (46) and (48) when the flow rate is such that the uniform state is unstable, is being considered by the authors at present.

To confirm these results, (84) were integrated numerically using a Runge–Kutta–Merson method. The initial conditions were taken close to the equilibrium point $(\epsilon_0, 0)$, and determined by (85). The integrations were performed in both directions to ensure both end points were reached. In all cases shown, $\tilde{P}_0$ was taken as 0.1, $\epsilon_0 = 0.3$, $\tilde{F} = 0.05$, $\tilde{R} = 10$ and $n = 3$. Three cases with $\alpha = 0.05$, 0.1 and 0.2 are shown in figures 7(*a*, *b*, *c*), $\mathrm{d}E/\mathrm{d}Y$ being plotted against E.

7. Numerical solution of the nonlinear equations

Finally, the full nonlinear equations (46) and (48) were solved numerically for E and V, with step initial conditions. An implicit Crank–Nicolson finite-difference scheme was used, the resulting nonlinear algebraic difference equations being solved

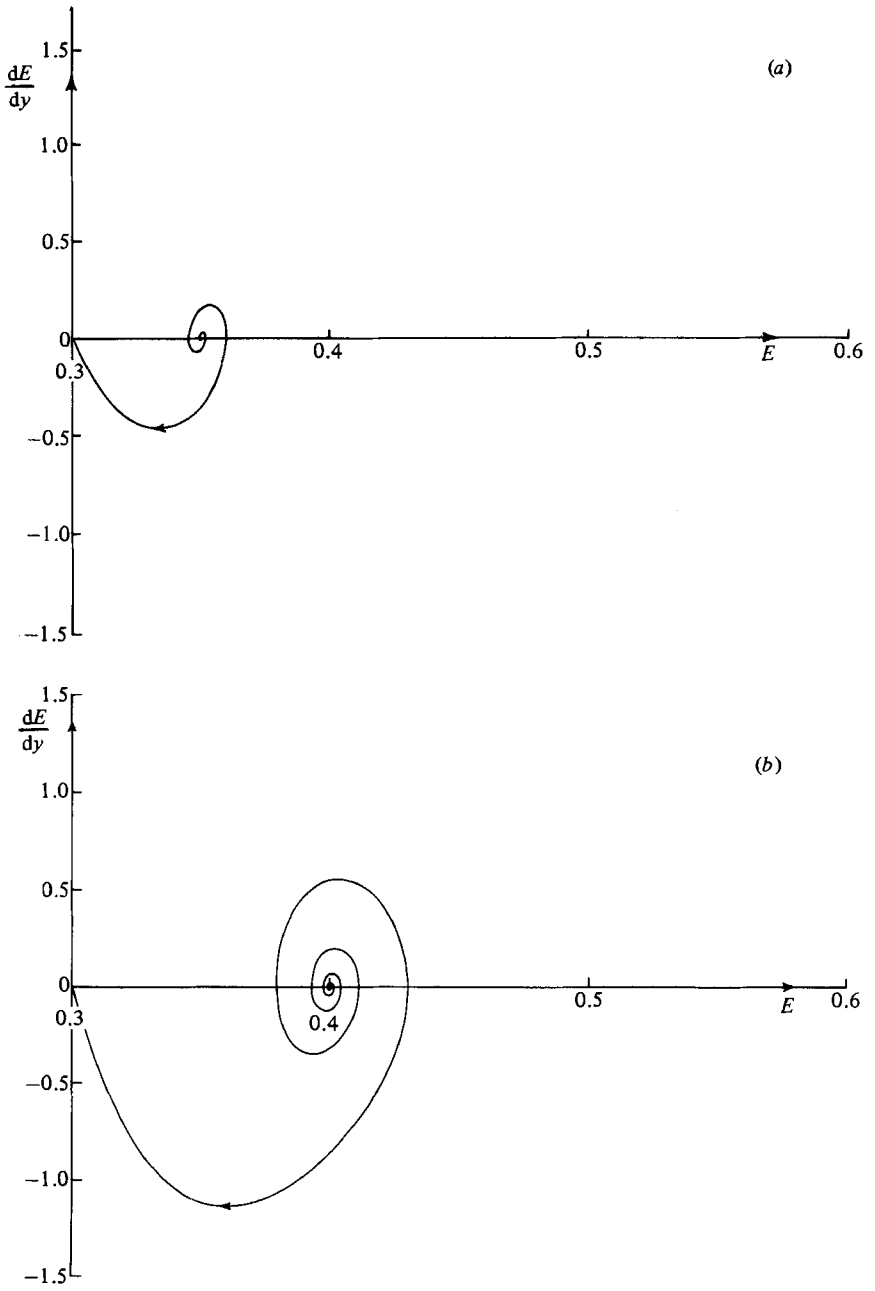

FIGURE 7 (*a*, *b*). For caption see facing page.

by iteration using the Newton–Raphson method. To smooth out the initial discontinuity, the initial conditions were taken as

$$E_{i,0} = \begin{cases} \epsilon_0 & (x > 1), \\ \epsilon_0 + \alpha \cos^2 \tfrac{1}{2}\pi x & (0 \leqslant x \leqslant 1), \\ \epsilon_0 + \alpha & (x < 0), \end{cases}$$

$$V_{i,0} = 0.$$

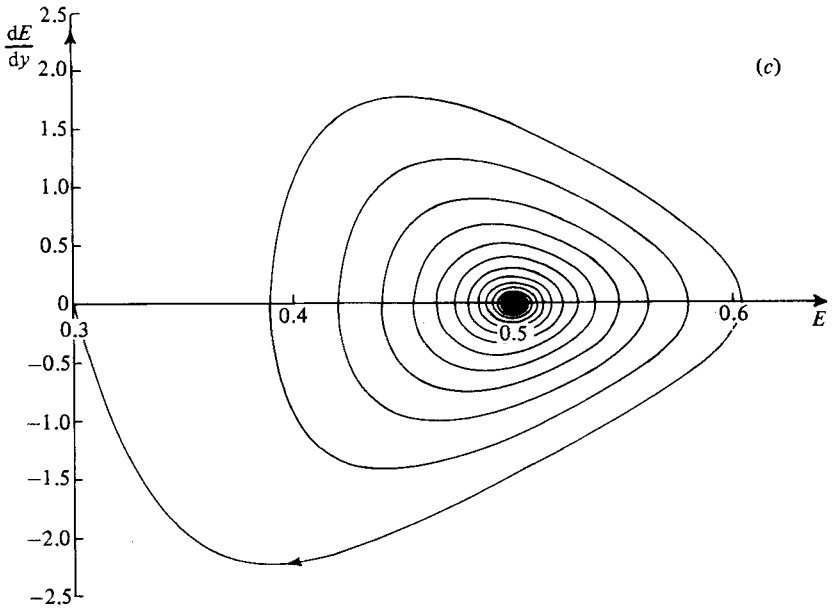

FIGURE 7. Graphs of $\mathrm{d}E/\mathrm{d}Y$ against E when: (*a*) $\epsilon_0 = 0.3$, $\tilde{F} = 0.05$, $\tilde{P}_0 = 0.1$, $\tilde{R} = 10.0$, $\alpha = 0.05$; (*b*) $\epsilon_0 = 0.3$, $\tilde{F} = 0.05$, $\tilde{P}_0 = 0.1$, $\tilde{R} = 10.0$, $\alpha = 0.1$; (*c*) $\epsilon_0 = 0.3$, $\tilde{F} = 0.05$, $\tilde{P}_0 = 0.1$, $\tilde{R} = 10.0$, $\alpha = 0.2$.

ϵ_0 was fixed at 0.3, $\tilde{P}_0$ at 0.08, which gives $E^{\mathrm{L}} = 0.53$ and $E^{\mathrm{u}} = 0.91$, and α was considered in the range $\epsilon_0 < \epsilon_0 + \alpha < E^{\mathrm{L}}$. The results compared well with the qualitative behaviour predicted using the approximate governing equation (53). The initial voidage distribution went through a transition period, and reached a quasisteady state when $t \approx 20$. For fixed $\tilde{F}$ and $\tilde{R}$ and sufficiently small α, the quasisteady transition from $\epsilon_0 + \alpha$ behind to ϵ_0 ahead was monotonic, while on increasing α, as $\epsilon_0 + \alpha$ approached E^{L}, oscillations appeared behind as $E \to \epsilon_0 + \alpha$. When oscillations were present, the lengthscale over which they decayed decreased with increasing $\tilde{R}$ for fixed α, while for fixed $\tilde{R}$ it increased with increasing α. The wavelength of the oscillations decreased with increasing $\tilde{R}$ and increased with increasing $\tilde{F}$ for fixed α. Three cases are shown in figures 8(*a–c*) in which $\tilde{R}$ and $\tilde{F}$ were fixed and α increased. Each case was stepped forward in time until a quasisteady state was reached, the initial and final states being shown. With $\alpha = 0.05$ the transition is monotonic, while for $\alpha = 0.1, 0.2$, oscillations appear behind the transition region.

8. Conclusions

By considering the evolution of a localized voidage disturbance imposed on an otherwise uniformly fluidized bed for which $F \ll 1$ (i.e. $U_0^2 \ll gh$) we have been able to determine the dominant effects of the many terms in the continuum equations of motion governing such a fluidized bed.

For small perturbations the equations of motion were linearized, and by considering the solution of the initial-value problem as a parameter expansion in powers of F, a uniformly valid leading-order approximation was found to be governed by the equation

$$\frac{\partial \bar{E}}{\partial t} + C_0 \frac{\partial \bar{E}}{\partial x} = F\left\{\psi_0 \frac{\partial^2 \bar{E}}{\partial x^2} - \frac{\eta_0}{R}\frac{\partial^3 \bar{E}}{\partial x^3}\right\}.$$

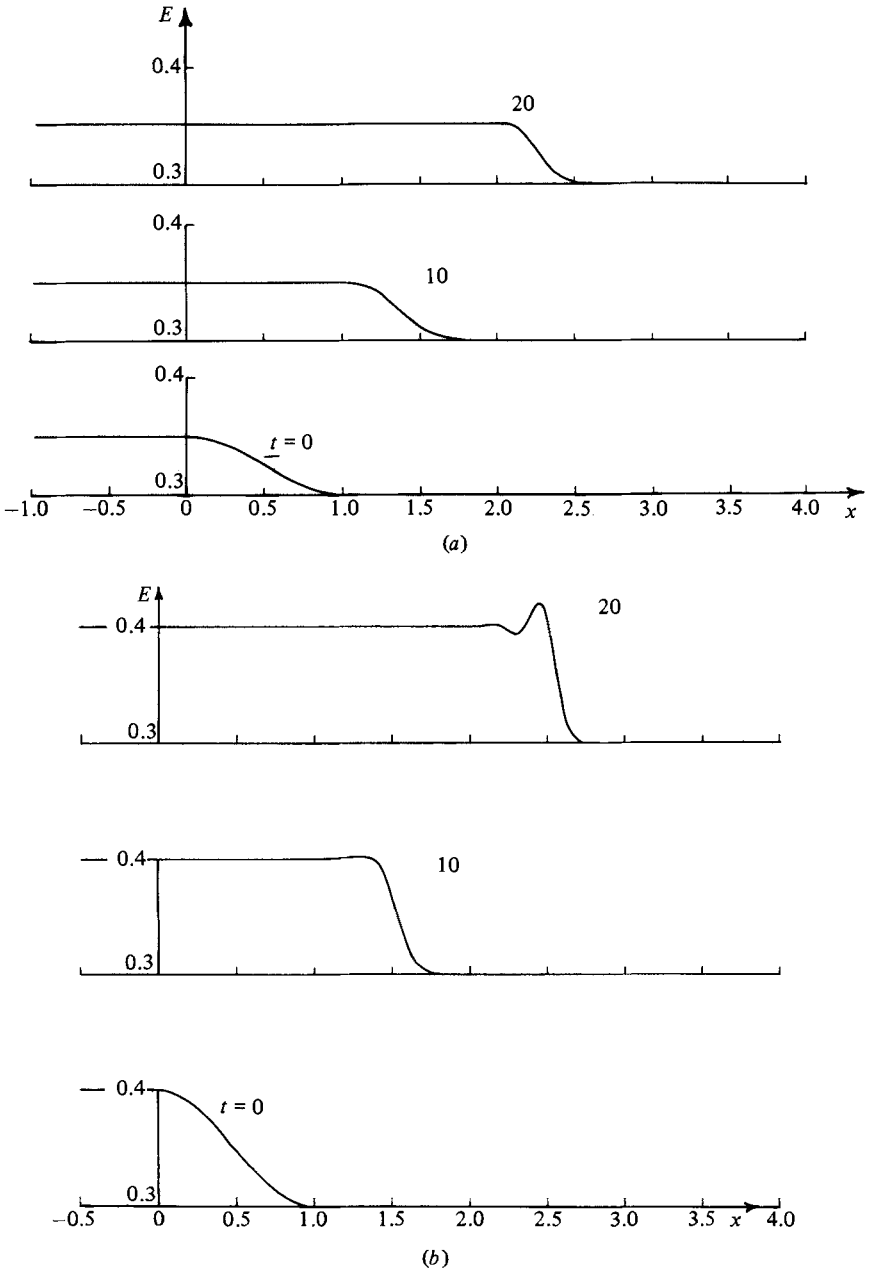

FIGURE 8(*a*, *b*). For caption see facing page.

From this equation the stability condition $\psi_0 > 0$ was found to depend upon both flow rate of the uniform state and the effect of particle-phase collisional pressure, and for $\psi_0 < 0$ the instability was shown to arise through a 'focusing' of voidage due to the negative diffusion coefficient, while the effect of particle-phase viscosity is dispersive. Further, the evolution was found to take place on three timescales. When t is $O(F)$ there is rapid adjustment in particle and fluid velocities, which propagate vertically upwards through the bed when t is $O(1)$, the effects of diffusion and dispersion being felt when t is $O(F^{-1})$. When the uniform state is stable, the initial

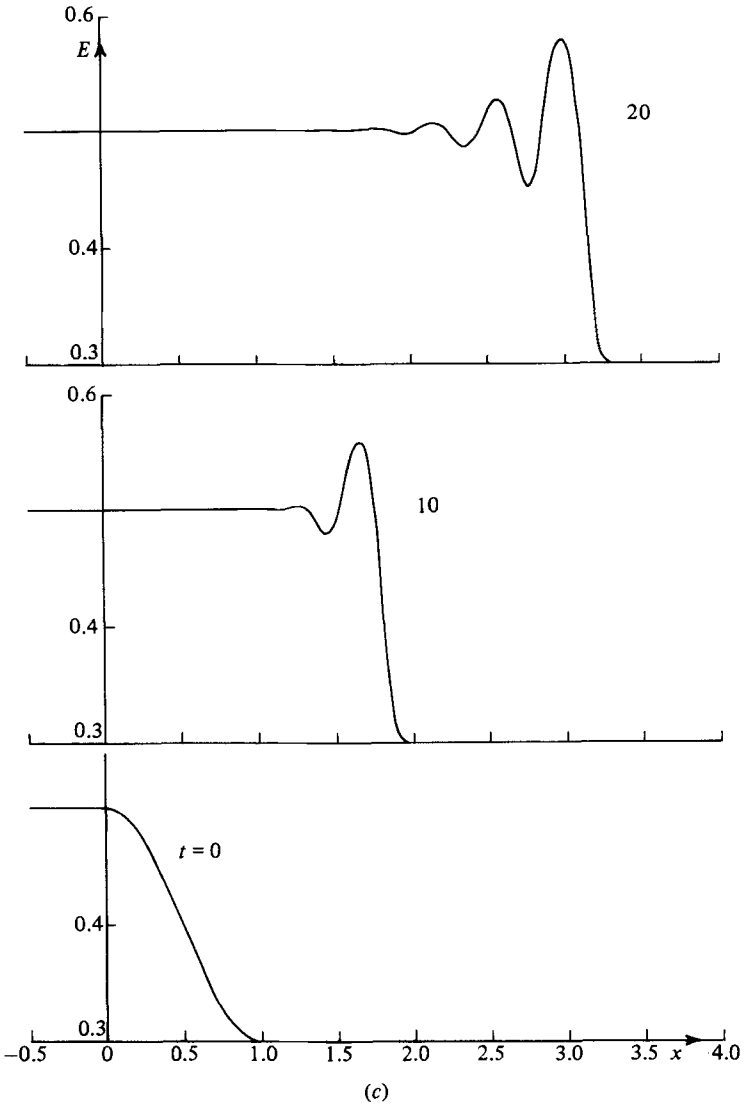

FIGURE 8. Graphs of E against x at $t = 0$, 10 and 20 when: (*a*) $\epsilon_0 = 0.3$, $\tilde{F} = 0.5$, $\tilde{R} = 10.0$, $\tilde{P}_0 = 0.08$, $\alpha = 0.05$; (*b*) $\epsilon_0 = 0.3$, $\tilde{F} = 0.5$, $\tilde{R} = 10.0$, $\tilde{P}_0 = 0.08$, $\alpha = 0.1$; (*c*) $\epsilon_0 = 0.3$, $\tilde{F} = 0.5$, $\tilde{R} = 10.0$, $\tilde{P}_0 = 0.08$, $\alpha = 0.2$.

disturbance was shown to develop into a decaying pulse followed by a decaying wavetrain.

For finite-amplitude disturbances, nonlinear effects were considered. The lower-order approximation, discussed for single-hump initial conditions, gave rise to voidage discontinuities after a finite time, at the front, rear or both depending upon the flow rate of the uniform state and the amplitude of the initial disturbance. Higher-order effects were then considered through an approximate equation for voidage, derived by neglecting terms $O(\tilde{F}^2)$. It was found that discontinuities arising in the lower-order approximation could be smoothed out by considering higher-order terms only for flow rates at which the uniform state is stable (stable on the linearized

theory), and provided that the initial amplitude $\epsilon_0 + \alpha$ was less than the lower critical value E^{L} if $\epsilon_0 < E^{\mathrm{L}}$, or greater than the upper critical value E^{u}, if $\epsilon_0 > E^{\mathrm{u}}$.

Finally, a detailed study of how the discontinuity structure behaves as $\epsilon_0 + \alpha \to E^{\mathrm{L}}$, and 'breaks down' as $\epsilon_0 + \alpha$ passes through E^{L}, indicates that, at flow rates for which the uniform state is unstable, the bed may restabilize at a quasisteady periodic state. This possibility is being pursued by the authors at present.

The authors would like to thank Professor C. McGreavy for his help with the preparation of this paper. One of the authors (D.J.N.) was in receipt of a S.E.R.C. Engineering Mathematics Research Studentship.

We would also like to thank the referees for their useful and interesting comments, which we hope have led to an overall improvement in the paper.

REFERENCES

Anderson, T. B. & Jackson, R. 1967 *Ind. Engng Chem. Fund.* **6**, 527.

Anderson, T. B. & Jackson, R. 1968 *Ind. Engng Chem. Fund.* **7**, 12.

Drew, D. A. & Segal, L. A. 1971 *Stud. Appl. Maths* **50**, 205.

Fanucci, J. B., Ness, N. & Yen, R. 1979 *J. Fluid Mech.* **94**, 353.

Garg, S. K. & Pritchett, J. W. 1975 *J. Appl. Phys.* **46**, 4493.

Homsy, G. M., El-Kaissey, M. M. & Didwania, A. 1980 *Int. J. Multiphase Flow* **6**, 305.

Murray, J. D. 1965 *J. Fluid Mech.* **21**, 465.

Nayfeh, A. H. 1973 *Perturbation Methods.* Wiley-Interscience.

Richardson, J. F. 1971 In *Fluidization* (ed. J. F. Davidson & D. Harrison). Academic.

Saffman, P. G. 1973 *Stud. Appl. Maths* **15**, 115.

Whitham, G. B. 1974 *Linear and Nonlinear Waves.* Wiley-Interscience.

Zenz, F. A. 1971 In *Fluidization* (ed. J. F. Davidson & D. Harrison). Academic.

Zenz, F. A. & Othmer, D. F. 1960 *Fluidization and Fluid–Particle Systems.* Reinhold.